Journal of

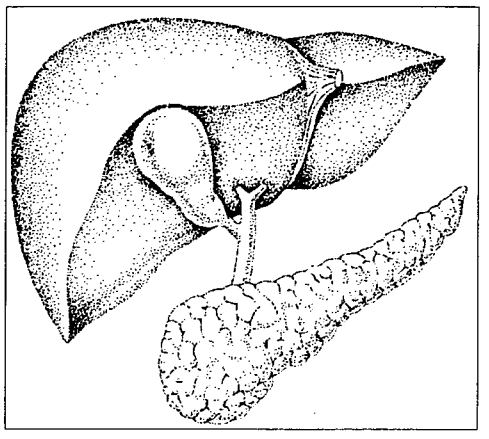

Hepato-Biliary-Pancreatic Surgery

Springer

Volume 14 Number 6 2007

J Hepatobiliary Pancreat Surg (2007) 14:586–589
DOI 10.1007/s00534-006-1218-x

Journal of HBP Surgery

Cystic endocrine tumor of the pancreas with an atypical multilocular appearance

Masatoshi Kajiwara[1], Naoto Gotohda[1], Masaru Konishi[1], Toshio Nakagohri[1], Shinichiro Takahashi[1], Motohiro Kojima[2], Takahiro Hasebe[3], and Taira Kinoshita[1]

[1] Department of Hepatobiliary Pancreatic Surgery, National Cancer Center Hospital East, 6-5-1 Kashiwanoha, Kashiwa, Chiba 277-8577, Japan
[2] Pathology Division, Research Center for Innovative Oncology, National Cancer Center Hospital East, Kashiwa, Chiba, Japan
[3] Surgical Pathology Section, Clinical Laboratory Division, National Cancer Center Hospital East, Kashiwa, Chiba, Japan

Abstract
A 46-year-old woman with epigastric pain was found to have a cystic tumor in the pancreas head on radiological examinations. The tumor was hypervascular, and its multilocular appearance resembled the "honeycomb" pattern of serous cystic tumor (SCT). The patient underwent surgery. The cut surface of the tumor showed a thick fibrous capsule with multiple cystic components, which contained necrotic tissue and brownish serous fluid, indicating an episode of hemorrhage. The cut surface of the tumor resembled solid-pseudopapillary tumor (SPT) on gross appearance. On immunohistochemical staining, the tumor cells showed diffuse and strong staining for synaptophysin (SYN), chromogranin A (CGA), and grimelius, and no staining for α 1-antitrypsin or CD10. We finally made a diagnosis of pancreatic endocrine tumor (PET). As PET sometimes shows an atypical multicystic appearance, immunohistochemical staining is mandatory for its correct diagnosis.

Key words Cystic endocrine tumor · Pancreas · Multilocular · Immunohistochemical staining

Introduction

Pancreatic endocrine tumor (PET) usually has a solid appearance, but it sometimes exhibits cystic components, especially in large lesions. Degenerative changes, such as hemorrhage and necrosis within the tumor during its growth, lead to the formation of cystic components.[1] If a cystic lesion is small enough, it is easy to make a correct diagnosis of PET. However, in cases in which the cystic components are intricate or occupy most of the tumor, it is sometimes difficult to distinguish it from other cystic tumors of the pancreas, such as solid-pseudopapillary tumor (SPT), mucinous cystic tumor (MCT), and serous cystic tumor (SCT).

This is a case report of a multicystic PET, which was preoperatively diagnosed as SCT and whose cut surface resembled SPT on gross appearance. We reached the correct diagnosis by performing immunohistochemical staining.

Case report

A 46-year-old woman presented with recurrent episodes of epigastric pain. She had had a history of bronchial asthma as a child, but was no longer on medication. She had no significant family history. On physical examination, no tumor was palpable in her abdomen. Laboratory test results, including amylase level, liver function, and carbohydrate antigen (CA) 19-9 and carcinoembryonic antigen (CEA) levels, were all within normal limits. Abdominal ultrasonography (US) revealed a well-circumscribed, multilocular cystic mass in the head of the pancreas that measured up to 6 cm in diameter. Endoscopic ultrasound examination (EUS) showed the structure of the tumor more clearly, and multiple cysts of variable size resembled the "honeycomb" appearance of SCT (Fig. 1a). Computed tomography (CT) demonstrated a 6-cm mass in the head of the pancreas; the mass was encapsulated by a thick wall, with calcification in the precontrast phase (Fig. 1b,c). The wall, septum, and solid components of the tumor were highly enhanced by contrast medium (Fig. 1d,e). Neither liver metastasis nor lymph node involvement around the pancreas was detected. After the CT examination, a skin rash emerged on her whole body, so further examination using contrast medium (angiography or endoscopic retrograde cholangiopancreatography [ERCP]) was not performed. On magnetic resonance imaging (MRI), the tumor showed heterogeneous low intensity on T1-weighted images

Offprint requests to: N. Gotohda
Received: November 17, 2006 / Accepted: December 27, 2006

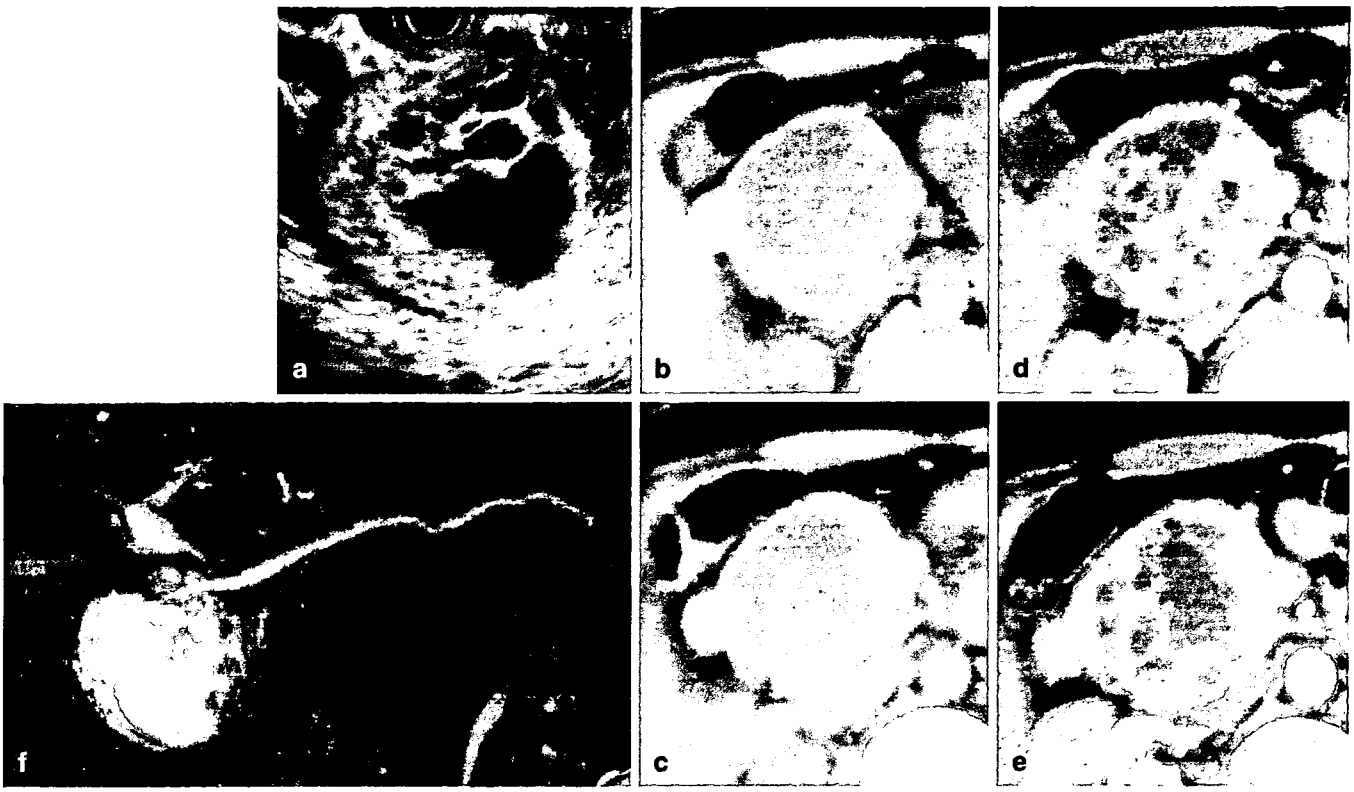

Fig. 1. **a** Endoscopic ultrasound (EUS) examination showed multiple cysts of variable size, which resembled the "honeycomb" appearance of a serous cystic tumor (SCT). **b, c** Computed tomography (CT) demonstrated a 6-cm mass in the head of the pancreas, encapsulated by a thick wall, with calcification in the precontrast phase. **d, e** On CT, the wall, septum, and solid components of the tumor were highly enhanced by contrast medium. **f** Magnetic resonance cholangiopancreatography (MRCP) revealed that the main pancreatic duct (MPD) and common bile duct (CBD) were compressed by the tumor and showed mild dilatation distally

and spotty high signal intensity, in concordance with the cystic components, on T2-weighted images. Magnetic resonance cholangiopancreatography (MRCP) revealed that the main pancreatic duct (MPD) and common bile duct (CBD) were compressed by the tumor and showed mild dilatation distally (Fig. 1f).

With a presumptive diagnosis of SCT, the patient underwent sub-total stomach-preserving pancreaticoduodenectomy (SSpPD). The postoperative course was uneventful and she was discharged on the fourteenth postoperative day. Six months after the surgery, she is alive without any evidence of recurrence.

Macroscopically, the tumor was round and elastic hard, measuring 7.5 × 7.0 × 6.5 cm. The cut surface showed a thick fibrous capsule with multiple cystic components, which contained necrotic tissue and brownish serous fluid, indicating an episode of hemorrhage (Fig. 2a). The gross appearance of the cut surface of the tumor resembled an SPT.

Microscopic examination revealed that the tumor was extensively vascularized, with areas of hemorrhage and necrosis, and a moderate amount of stroma. The tumor cells were medium-sized and their nuclei were round and uniform. No mitosis was detected. The tumor cells were arranged mainly in a trabecular pattern. In some areas, however, the tumor cells were separated by stroma and showed a pseudopapillary-like pattern (Fig. 2b,c). There was no lymph node metastasis around the tumor. Neither extracapsular invasion nor blood vessel invasion was detected. For discrimination between SPT and PET, immunohistochemical examination was performed. The tumor cells showed diffuse and strong staining for synaptophysin (SYN; Fig. 2d), chromogranin A (CGA; Fig. 2e), and grimelius (Fig. 2f), and weak staining for AE1/AE3. However, there was no staining for α 1-antitrypsin or CD10 (Fig. 2g). The morphologic appearance and immunohistochemical profile were compatible with PET. To evaluate the malignant potential of this tumor, we checked the MIB-1 index, and it was less than 1%.

Discussion

Pancreatic endocrine tumor (PET) usually shows a solid pattern, but it sometimes exhibits cystic components,

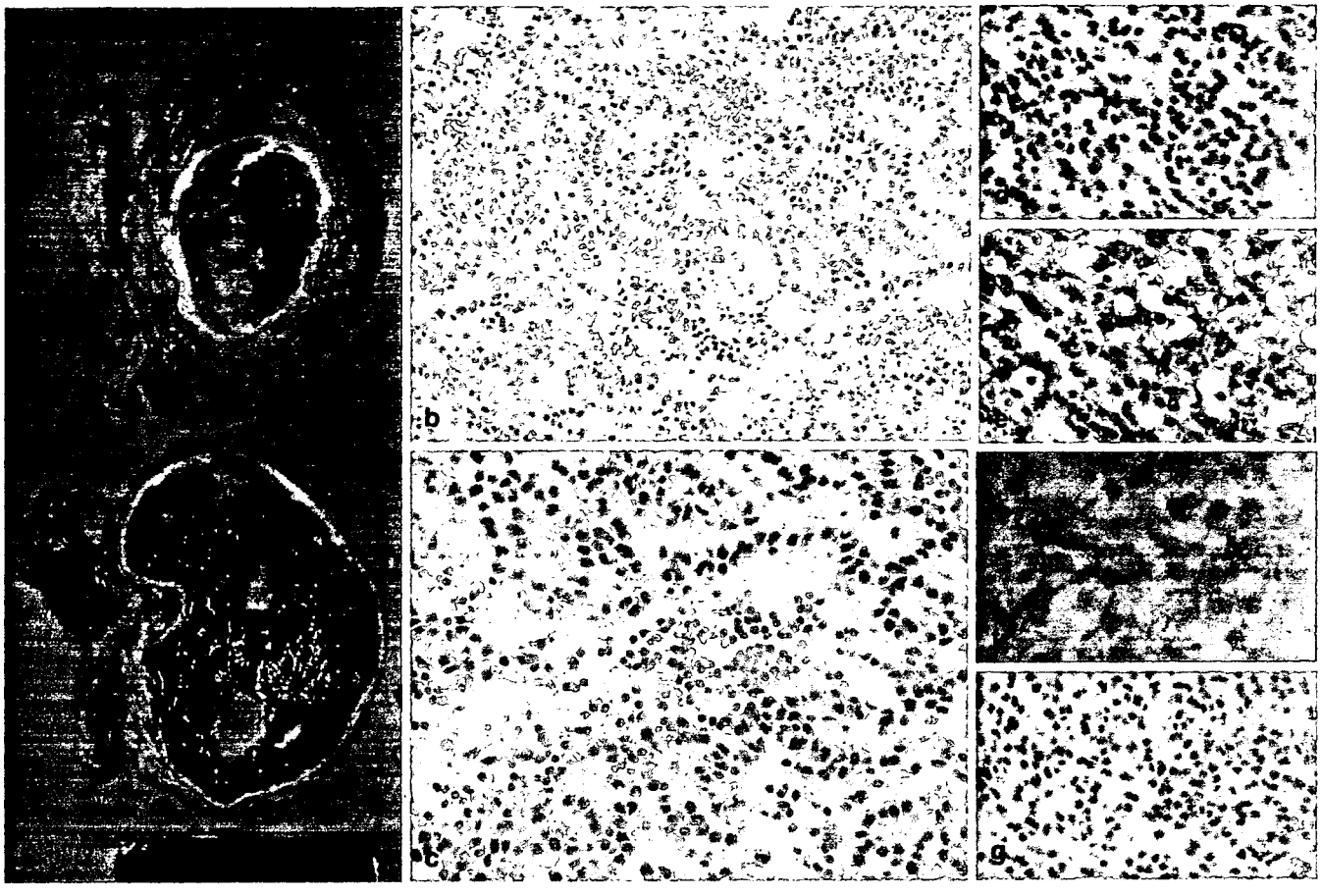

Fig. 2. **a** Macroscopically, the cut surface of the tumor showed a thick fibrous capsule with multiple cystic components. Its gross appearance resembled a solid-pseudopapillary tumor (SPT). **b, c** Microscopically, the tumor cells were arranged in a trabecular pattern. In some areas, however, the tumor cells showed a pseudopapillary-like pattern. **d, e, f, g** On immunohistochemical staining, the tumor cells showed diffuse and strong staining for synaptophysin (**d**), chromogranin A (**e**), and grimelius (**f**),and no staining for CD10 (**g**). **b** H&E, ×100; **c** H&E, ×200; **d** ×200; **e** ×200; **f** ×400; **g** ×200

especially in large lesions. The formation of cystic components within PET seems to be due to hemorrhage and necrosis of the tumor during its growth.[1] These degenerative changes are sometimes accompanied by the formation of a fibrous capsule around the tumor, which reduces its vascularization and promotes ischemic changes.[2]

Most cystic PETs are reported to be nonfunctioning tumors which do not produce enough hormone to produce clinical symptoms, whereas functioning tumors such as gastrinomas and insulinomas are usually detected at a small size because of their characteristic clinical manifestations.[2,3]

Cystic PET, of course, has the same radiological characteristics as the common solid type of PET, such as hypervascularity and the presence of calcification. Furthermore, cystic PET is reported to have unique radiographic findings such as thickening of the cyst wall and irregularity of the inner surface.[4] These structures are well-enhanced on post-contrast CT or MRI. The cystic components of PET vary in size and number. They are sometimes unilocular and sometimes multilocular. If the cystic lesion is small enough, it is possible to reach the correct diagnosis of PET from its characteristic radiological appearance, as mentioned above. However, when it shows a complicated cystic pattern, cystic PET can be misdiagnosed as other cystic tumors of the pancreas, such as SPT, SCT, and MCT.

Ligneau et al.[5] reported that 7 of 13 cystic PETs showed a microcystic appearance, and 2 of the 7 were diagnosed as SCT preoperatively. Gerke et al.[6] reported a case of a nonfunctioning PET that had the typical microcystic "honeycomb" appearance of SCT on preoperative imaging. Similarly, our initial diagnosis in the present patient was SCT, as the tumor was hypervascular, and its multilocular appearance resembled the "honeycomb" pattern of SCT. The thickness of the wall of the tumor, however, was not typical of SCT, which, in retrospect, we should have noted. Some other case reports have also indicated difficulties in making a diag-

nosis of cystic pancreatic tumors preoperatively owing to the variation in their appearance.[7,8]

The gross appearance of the tumor in our patient mimicked that of SPT. The tumor had a thick fibrous capsule, consisted of solid and cystic components, and contained necrotic tissue and brownish serous fluid, which indicated a hemorrhagic episode. It is thought that degenerative changes, such as necrosis and hemorrhage, occurred multifocally within the tumor during its growth, followed by the formation of the cystic components.

Microscopically, round, uniform tumor cells were arranged in a trabecular pattern. As they were separated by loose fibrous stroma, they displayed a pseudopapillary-like pattern in some areas. SPT often shows endocrine differentiation, and is sometimes positive for endocrine markers such as neuron-specific enolase (NSE) and SYN.[9] On immunohistochemical staining to differentiate PET from SPT, Notohara et al.[9] reported that CD10 and neuroendocrine markers, such as CGA and SYN, were useful. They reported that all SPTs they investigated had strong reactivity for CD10, whereas 95% of the PETs were negative or only focally positive for CD10. All the SPTs were negative for CGA. On the other hand, all the PETs demonstrated positive reactivity for CGA.

In our patient, the tumor cells showed diffuse and strong staining for CGA, and no staining for CD10. Thus, we finally made a diagnosis of cystic PET. We did not perform immunohistochemical staining for insulin, glucagon, somatostatin, or pancreatic polypeptide. According to the recent World Health Organization (WHO) criteria,[10] this case was classified as well-differentiated endocrine tumor with uncertain behavior, because it did not have any lymph node metastasis, local invasion, blood vessel invasion, or mitosis, and its MIB-1 index was less than 2%, but the size of the tumor was greater than 2cm. Our patient will need close follow-up to monitor for recurrence.

We should be alerted that PET sometimes shows a multicystic appearance mimicking other pancreatic cystic tumor entities. Immunohistochemical staining is mandatory for the correct diagnosis of PET.

References

1. Davtyan H, Nieberg R, Reber HA. Pancreatic cystic endocrine neoplasms. Pancreas 1990;5:230–3.
2. Iacono C, Serio G, Fugazzola C, Zamboni G, Bergamo Andreis IA, Jannucci A, et al. Cystic islet cell tumors of the pancreas. A clinico-pathological report of two nonfunctioning cases and review of the literature. Int J Pancreatol 1992;11:199–208.
3. Buetow PC, Parrino TV, Buck JL, Pantongrag-Brown L, Ros PR, Dachman AH, et al. Islet cell tumors of the pancreas: pathologic-imaging correlation among size, necrosis and cysts, calcification, malignant behavior, and functional status. AJR Am J Roentgenol 2002;165:1175–9.
4. Takeshita K, Furui S, Makita K, Yamauchi T, Irie T, Tsuchiya K, et al. Cystic islet cell tumors: radiologic findings in three cases. Abdom Imaging 1994;19:225–8.
5. Ligneau B, Lombard-Bohas C, Partensky C, Valette PJ, Calender A, Dumortier J, et al. Cystic endocrine tumors of the pancreas: clinical, radiologic, and histopathologic features in 13 cases. Am J Surg Pathol 2001;25:752–60.
6. Gerke H, Byrne M, Xie HB, Paulson EK, Tyler DS, Baillie J, et al. A wolf in sheep's clothing: a non-functioning islet cell tumor of the pancreas masquerading as a microcystic (serous cystic) adenoma. JOP 2004;5:225–30.
7. Fujiwara H, Ajiki T, Fukuoka K, Mitsutsuji M, Yamamoto M, Kuroda Y. Macrocystic serous cystadenoma of the pancreas. J Hepatobiliary Pancreat Surg 2000;7:92–6.
8. Seki M, Ninomiya E, Aruga A, Yamada K, Koga R, Saiura A, et al. Image-diagnostic features of mature cystic teratomas of the pancreas: report on two cases difficult to diagnose preoperatively. J Hepatobiliary Pancreat Surg 2005;12:336–40.
9. Notohara K, Hamazaki S, Tsukayama C, Nakamoto S, Kawabata K, Mizobuchi K, et al. Solid-pseudopapillary tumor of the pancreas: immunohistochemical localization of neuroendocrine markers and CD10. Am J Surg Pathol 2000;24:1361–71.
10. Heitz PU, Komminoth P, Perran A, Klimstra DS, Dayal Y, Bordi C, et al. Tumor of the endocrine pancreas. In: Delellis RA, Lloyd RV, Heitz PU, Eng C, editors. World Health Organization classification of tumors: pathology and genetics of tumors of endocrine organs. Lyon: IARC; 2004. p. 175–208.

Regression of intestinal adenomas by vaccination with heat shock protein 105-pulsed bone marrow-derived dendritic cells in $Apc^{Min/+}$ mice

Kazunori Yokomine,[1,2] Tetsuya Nakatsura,[1,3] Satoru Senju,[1] Naomi Nakagata,[4] Motozumi Minohara,[5] Jun-ichi Kira,[5] Yutaka Motomura,[1,3] Tatsuko Kubo,[6] Yutaka Sasaki[2] and Yasuharu Nishimura[1,7]

Departments of [1]Immunogenetics and [2]Gastroenterology and Hepatology, Graduate School of Medical Sciences, Kumamoto University, 1-1-1 Honjo, Kumamoto 860-8556; [3]Immunotherapy Section, Investigative Treatment Division Research Center for Innovative Oncology, National Cancer Center Hospital East, 6-5-1 Kashiwanoha, Kashiwa 277-8577; [4]Center for Animal Resources and Development, Kumamoto University, 2-2-1 Honjo, Kumamoto 860-0811; [5]Department of Neurology, Neurological Institute, Graduate School of Medical Sciences, Kyushu University, 3-1-1 Maidashi, Higashi-ku, Fukuoka 812-8582; [6]Department of Molecular Pathology, Graduate School of Medical Sciences, Kumamoto University, 1-1-1 Honjo, Kumamoto 860-8556, Japan

(Received May 12, 2007/Revised August 6, 2007/Accepted August 7, 2007/Online publication September 24, 2007)

Heat shock protein (HSP) 105 is overexpressed in various cancers, but is expressed at low levels in many normal tissues, except for the testis. A vaccination with HSP105-pulsed bone marrow-derived dendritic cells (BM-DC) induced antitumor immunity without causing an autoimmune reaction in a mouse model. Because $Apc^{Min/+}$ mice develop multiple adenomas throughout the intestinal tract by 4 months of age, the mice provide a clinically relevant model of human intestinal tumor. In the present study, we investigated the efficacy of the HSP105-pulsed BM-DC vaccine on tumor regression in the $Apc^{Min/+}$ mouse. Western blot and immunohistochemical analyses revealed that the tumors of the $Apc^{Min/+}$ mice endogenously overexpressed HSP105. Immunization of the $Apc^{Min/+}$ mice with a HSP105-pulsed BM-DC vaccine at 6, 8, and 10 weeks of age significantly reduced the number of small-intestinal polyps accompanied by infiltration of both $CD4^+$ and $CD8^+$ T cells in the tumors. Cell depletion experiments proved that both $CD4^+$ and $CD8^+$ T cells play a critical role in the activation of antitumor immunity induced by these vaccinations. These findings indicate that the HSP105-pulsed BM-DC vaccine can provide potent immunotherapy for tumors that appear spontaneously as a result of the inactivation of a tumor suppressor gene, such as in the $Apc^{Min/+}$ mouse model. (*Cancer Sci* 2007; 98: 1930–1935)

Colorectal cancer is the third most common cancer and the fourth most frequent cause of cancer death worldwide. Every year, more than 945 000 people develop colorectal cancer worldwide, and approximately 492 000 patients die.[1] For patients with advanced stages of colorectal cancer, adjuvant systemic chemotherapy is a standard treatment. Major progress has been made by the introduction of regimens containing new cytotoxic drugs such as irinotecan and oxaliplatin; however, the new therapeutic regimens have led to only 8–9 months of progression-free survival.[2] Consequently, the development of new and effective therapeutic approaches, such as immunotherapy, is needed to expand treatment options.

The progression from normal epithelium to colorectal cancer is a multistep process involving the accumulation of multiple genetic alterations.[3] The *APC* gene, a tumor suppressor, is considered to be a gatekeeper in colon tumorigenesis,[4] and one of the earliest molecular events is the loss of function of the *APC* gene product.[5] APC forms a multimeric complex with the axis inhibition protein (AXIN)2 and glycogen synthase kinase 3β, which regulates the nuclear accumulation of β-catenin, a signal transducer of the wnt pathway.[6] When the APC–β-catenin complex is destabilized because of *APC* mutations, β-catenin binds and activates transcription factors that regulate the expression of potent oncogenes such as *c-Myc* and *c-Met*.[7] The importance of the *APC* gene product was confirmed by the demonstration that 80% of all sporadic colorectal cancers are characterized by one or more mutations in the *APC* gene, approximately 60% of which result in the expression of a truncated version of the APC protein.[8]

The $Apc^{Min/+}$ mouse has a nonsense mutation from T to A in the *Apc* gene at codon 850, homologous to the human germline and somatic *APC* mutation.[9] Although homozygous mice die before birth, all heterozygous mice develop multiple adenomas throughout their intestinal tract at an early age.[10] The $Apc^{Min/+}$ mouse model is unique in that tumors appear spontaneously in the intestinal tract, rather than as a result of induction by a carcinogen. This model is particularly advantageous for testing preventive agents targeted against early stage lesions because adenomas grow to a grossly detectable size within a few months on a defined genetic background.[10] Because $Apc^{Min/+}$ mice develop tumors due to the inactivation of the same tumor suppressor gene known to be involved in the pathogenesis of most colon cancers in humans, this model represents a clinically relevant model of human intestinal tumorigenesis.[10] Furthermore, germline mutations in the human *APC* gene cause FAP, whose symptoms resemble those of an $Apc^{Min/+}$ mouse. Therefore, this model provides useful information about not only colon cancer but also FAP.

Heat shock proteins are soluble intracellular proteins that are expressed ubiquitously, and their expression can be induced at much higher levels due to heat shock or other forms of stress. The essential functions of HSP are to bind and protect partially denatured proteins from further denaturation and aggregation.[11] A previous study reported that HSP105 (often called HSP110), identified with serological identification of antigens using the recombinant expression cloning (SEREX) method, is overexpressed in a variety of human cancers, including colorectal, pancreatic, thyroid, esophageal, and breast carcinoma, whereas HSP105 is expressed at lower levels in many normal tissues, except for the testis.[12,13] Immunotherapy targeted at HSP105 in the mouse prophylactic model, such as HSP105-pulsed BM-DC and *HSP105* DNA vaccines, induce antitumor immunity without causing an autoimmune reaction.[14,15] These findings indicate that HSP105 itself could be considered as a valuable tumor-associated antigen for immune-based treatment of various tumors.

[7]To whom correspondence should be addressed.
E-mail: mxnishim@gpo.kumamoto-u.ac.jp

Abbreviations: APC, adenomatous polyposis coli; BM-DC, bone marrow-derived dendritic cell; COX, cyclooxygenase; DC, dendritic cell; ELISPOT, enzyme-linked immunospot; FAP, familial adenomatous polyposis; HSP, heat shock protein; mAb, monoclonal antibody; MBP, myelin basic protein; MHC, major histocompatibility complex; PBS, phosphate-buffered saline.

doi: 10.1111/j.1349-7006.2007.00612.x

Another study reported that HSP105 is involved in tumorigenesis by protecting cancer cells from apoptosis.[16] The constitutive overexpression of HSP105 protein was found to be essential for various cancer cells to survive and, conversely, the apoptosis-inducing effect of HSP105 small interfering RNA (siRNA) is specific for cancer. In contrast, HSP can also stimulate an adaptive immune response against antigens bound to HSP,[17] provided that the vaccine forms a complex of recombinant HSP110 and target tumor-associated antigen.[18,19]

In the present study, $Apc^{Min/+}$ mice were used as a model of a cancer immunotherapy for human colorectal cancer. Because tumors in $Apc^{Min/+}$ mice strongly express HSP105, the efficacy of immunization with HSP105-pulsed BM-DC for preventing the development of tumors in $Apc^{Min/+}$ mice was investigated.

Materials and Methods

Mice and genotyping. Frozen embryos of $Apc^{Min/+}$ mice obtained from the Jackson Laboratory were transferred to C57BL/6J mice (purchased from Charles River Japan, Yokohama, Japan) at the Center for Animal Resources and Development, Kumamoto University. Mice at 4–5 weeks of age were characterized for the *Apc* genotype by polymerase chain reaction analysis of tail DNA with the use of allele-specific primers.[20] The concentrations of these primers were 1.0 μM (5′-TGAGAAAGACAGAAGTTA-3′), 1.0 μM (5′-TTCCACTTTGGCATAAGGC-3′), and 0.2 μM (5′-GCCATCCCTTCACGTTAG-3′). The amplification conditions were 5 min at 94°C before 35 cycles at 94°C for 1 min, 50°C for 1 min, and 72°C for 1 min, followed by a final extension at 72°C for 5 min. The mice were maintained by breeding male $Apc^{Min/+}$ mice to female C57BL/6J mice. The mice were kept under specific pathogen-free conditions and these experiments were approved by the Animal Research Committee of Kumamoto University.

Production of recombinant proteins. Highly purified recombinant mouse HSP105 was produced from *Escherichia coli* strain BL21 cells transduced with the mouse *HSP105* gene expression vector, as described previously.[14,21] We also produced highly purified recombinant MBP as a negative control, which was prepared from bacterial lysate in the same way as the preparation of recombinant HSP105. Both recombinant HSP105 and MBP were estimated to be almost endotoxin free using a Limulus amebocyte lysate assay kit (BioWhittaker, Walkersville, MD, USA), and the endotoxin contents in the materials were <10 endotoxin U/mg.

Immunizations and scoring of tumors. HSP105-pulsed BM-DC were prepared as described previously.[14,22] The mice were inoculated intraperitoneally with HSP105-pulsed BM-DC (5×10^5) suspended in 200 μL PBS at 6, 8, and 10 weeks of age. The mice were treated with BM-DC alone, MBP-pulsed BM-DC, or PBS as controls. At 12 weeks of age the mice were killed and their small intestines were removed and fixed with formaldehyde. The intestines were then opened and stained with methylene blue and the number of tumors was counted.

Western blot and immunohistochemical analysis. Western blotting and the immunohistochemical detection of HSP105 were carried out as described previously.[12,16] Rabbit polyclonal antihuman HSP105 (Santa Cruz Biotechnology, Santa Cruz, CA, USA) was used as the primary antibody in this study. The immunohistochemical staining of $CD4^+$ and $CD8^+$ T cells was carried out as described previously.[14] mAb specific to CD4 (L3T4; BD PharMingen, San Diego, CA, USA) and CD8 (Ly-2; BD PharMingen) were used for staining.

Depletion of $CD4^+$ or $CD8^+$ T cells in mice. Rat mAb GK1.5 specific to mouse CD4 and 2.43 specific to mouse CD8 were used to deplete $CD4^+$ and $CD8^+$ T cells, respectively, *in vivo*. The 6-week-old $Apc^{Min/+}$ mice were injected with ascites (500 μg/mouse) from hybridoma-bearing nude mice six times intraperitoneally with an interval of 3–4 days between injection. Normal rat IgG (Chemicon, Temecula, CA, USA) was used as a control. The depletion of T cell subsets was monitored by a flow cytometric analysis, which showed a more than 90% specific depletion in the number of splenocytes.

ELISPOT assay. The $Apc^{Min/+}$ mice were immunized with HSP105-pulsed BM-DC or BM-DC alone at 6 and 8 weeks of age. At 10 weeks of age, spleen cells were harvested and depleted of $CD4^+$ or $CD8^+$ T cells using a magnetic cell-sorting system with antimouse CD4 mAb and antimouse CD8a (Mittenyi Biotec GmbH, Bergisch Gladbach, Germany) mAb, respectively. The purity of these T-cell subsets exceeded 95% based on a flow cytometric analysis. $CD4^-$ T cells were used as a source of $CD8^+$ T cells and antigen-presenting cells, and $CD8^-$ T cells were used as a source of $CD4^+$ T cells and antigen-presenting cells. Five hundred thousand $CD4^-$ or $CD8^-$ T cells were added to each well in triplicate cultures of RPMI-1640 medium containing 10% fetal calf serum (FCS) together with 2 μg/mL HSP105, MBP, and one with medium only at 37°C for 24 h. Then ELISPOT assays were carried out as described previously.[12]

Statistical analysis. The statistical significance of differences between the experimental groups was determined using Student's *t*-test. The overall survival rate was calculated using the Kaplan–Meier method, and statistical significance was evaluated using Wilcoxon's test. A value of $P < 0.05$ was considered to be statistically significant.

Results

Overexpression of HSP105 in intestinal adenomas of the $Apc^{Min/+}$ mice. A previous study reported that mouse HSP105 is overexpressed in liver metastasis of a murine colorectal adenocarcinoma cell line (Colon26), and in lung metastasis of a murine melanoma cell line (B16-F10).[15] The expression of HSP105 in tumors of $Apc^{Min/+}$ mice were thereby analyzed. The small intestines of $Apc^{Min/+}$ mice were excised, and the expression level of HSP105 was evaluated by both western blot and immunohistochemical analyses. The $Apc^{Min/+}$ mice developed adenomatous polyps spontaneously, predominantly in and throughout the small intestine at 4 months of age (Fig. 1a). Both western blot and immunohistochemical analyses confirmed the strong expression of HSP105 in the tumors of $Apc^{Min/+}$ mice (Fig. 1b,c). Based on these observations, the $Apc^{Min/+}$ mouse was chosen as a murine model of cancer immunotherapy targeted at HSP105.

Immunization with HSP105-pulsed BM-DC vaccine reduced the number of small intestinal polyps in $Apc^{Min/+}$ mice. The preventive effects of HSP105-pulsed BM-DC vaccination on the development of adenomatous polyps in the $Apc^{Min/+}$ mice were investigated. The mice were divided into four groups consisting of 10 mice each, inoculated intraperitoneally with PBS (group 1), BM-DC (group 2), MBP-pulsed BM-DC (group 3), or HSP105-pulsed BM-DC (group 4) at 6, 8, and 10 weeks of age. Two weeks after the last immunization, the number of tumors in the small intestine was counted.

Tumors had already developed in the small intestine of $Apc^{Min/+}$ mice at the time of the first vaccination (6 weeks of age). Each mouse had a mean of 6.3 ± 3.4 tumors at that time. The mean number of tumors at 12 weeks of age was 20.9 ± 9.6 in group 4, which was significantly less ($P = 0.006$) than the numbers in group 1 (37.8 ± 11.0), group 2 (40.8 ± 11.0), and group 3 (34.8 ± 9.5) (Fig. 2a). It was therefore concluded that the HSP105-pulsed BM-DC vaccine has the potential to prevent the growth of tumors expressing HSP105. The survival time in group 4 (175.3 ± 32.6 days) tended to be longer than that in group 1 (146.7 ± 13.0 days) and in group 2 (152.7 ± 25.5 days); however, the difference between group 4 and group 2 was not statistically significant ($P = 0.081$; Fig. 2b). No apparent abnormalities, such as weight loss, hair abnormality, or paralysis, were observed in

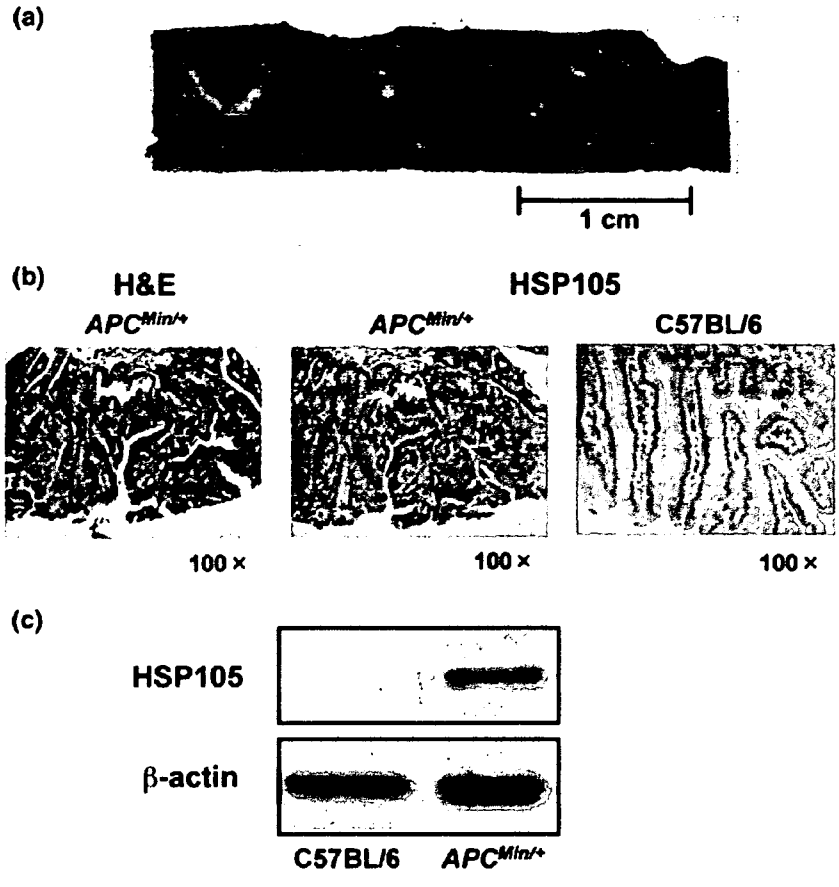

Fig. 1. Overexpression of heat shock protein (HSP) 105 in adenomatous polyps of $Apc^{Min/+}$ mice. (a) Macroscopic polyps in the small intestine of 4-month-old $Apc^{Min/+}$ mice. (b) A microscopic analysis of polyps in the small intestine of 12-week-old $Apc^{Min/+}$ mice stained with hematoxylin–eosin (left) and anti-HSP105 monoclonal antibody (middle). A normal small intestine was stained with anti-HSP105 monoclonal antibody as a negative control (right). Objective magnification was ×100. (c) Western blot analysis of HSP105 in the small intestine of 4-month-old $Apc^{Min/+}$ mice. The samples were small intestines of $Apc^{Min/+}$ and C57BL/6J mice homogenized in lysis buffer. The small intestines of three mice per group were pooled.

the mice immunized with HSP105-pulsed BM-DC, suggesting that serious autoimmunity was not observed in the mice. A histological analysis of the major organs (brain, lung, heart, liver, small intestine, kidney, and testis) of the immunized mice revealed no pathological inflammation (data not shown).

Both CD4⁺ and CD8⁺ T cells are required for antitumor immunity. To determine the role of $CD4^+$ and $CD8^+$ T cells in the reduction of tumor development in $Apc^{Min/+}$ mice immunized with HSP105-pulsed BM-DC, mice were depleted of $CD4^+$ or $CD8^+$ T cells by treatment with anti-CD4 or anti-CD8 mAb, respectively, *in vivo*. During the depletion procedure, the mice were immunized with PBS or HSP105-pulsed BM-DC vaccine (Fig. 3a). In the group of mice immunized with HSP105-pulsed BM-DC, together with inoculation of anti-CD4 mAb (35.5 ± 10.8) or anti-CD8 mAb (30.2 ± 9.6), the tumor numbers were significantly larger than those in the mice given rat IgG (18.8 ± 5.9) or left untreated (19.9 ± 7.7). The differences in the tumor numbers between the anti-CD4 mAb-treated group and the rat IgG-treated group ($P = 0.002$), and between the anti-CD8 mAb-treated group and the rat IgG-treated group ($P = 0.013$) were statistically significant. In the group of mice inoculated with PBS, the numbers of tumors in the mice given either anti-CD4 mAb (38.1 ± 5.7) or anti-CD8 mAb (38.1 ± 5.6) did not differ significantly from those in the mice given rat IgG (37.8 ± 4.8) or in the untreated mice (40.8 ± 6.1) (Fig. 3b). These results suggest that both $CD4^+$ and $CD8^+$ T cells play a crucial role in the protective antitumor immunity induced by the HSP105-pulsed BM-DC vaccine, because the HSP105-pulsed BM-DC vaccine was not effective in the mice showing a depletion of either $CD4^+$ or $CD8^+$ T cells.

Detection of HSP105-specific T cells in mice immunized with the HSP105-pulsed BM-DC vaccine. The $Apc^{Min/+}$ mice were immunized with HSP105-pulsed BM-DC or BM-DC at 6 and 8 weeks of age. At 10 weeks of age, spleen cells were harvested and depleted of $CD4^+$ or $CD8^+$ T cells using magnetic cell-sorting system, and the ELISPOT assay was carried out. The ELISPOT assay showed that the $CD8^-$ cells ($CD4^+$ T cells and antigen-presenting cells) derived from the mice immunized with HSP105-pulsed BM-DC produced a significantly larger amount of interferon-γ in response to HSP105 than did $CD8^-$ cells derived from mice immunized with BM-DC. Similar results were observed for the $CD4^-$ cells ($CD8^+$ T cells and antigen-presenting cells) (Fig. 4a). These observations clearly indicate that both HSP105-specific $CD4^+$ and $CD8^+$ T cells were induced in the mice immunized with HSP105-pulsed BM-DC vaccine.

To investigate the antitumor effect of the HSP105-pulsed BM-DC vaccination, the tumor was evaluated histopathologically. The small intestines derived from the mice used for the ELISPOT assay were stained with anti-CD4 or anti-CD8 mAb. Both $CD4^+$ and $CD8^+$ T cells infiltrated into the tumors of mice immunized with HSP105-pulsed BM-DC; however, this was not the case in tumors derived from the mice immunized with BM-DC (Fig. 4b). These results suggest that HSP105-pulsed BM-DC have the potential to sensitize many HSP105-specific $CD4^+$ and $CD8^+$ T cells to kill tumor cells.

Discussion

In the present study, the HSP105-pulsed BM-DC vaccine could sensitize HSP105-specific T cells *in vivo* and inhibited the spontaneous development of intestinal tumors overexpressing HSP105 in $Apc^{Min/+}$ mice. For diseases of germline mutations that cause malignancy throughout the body, such as FAP, novel strategies for the prevention of cancer are needed urgently because there is no satisfactory treatment for FAP. Therefore,

doi: 10.1111/j.1349-7006.2007.00612.x

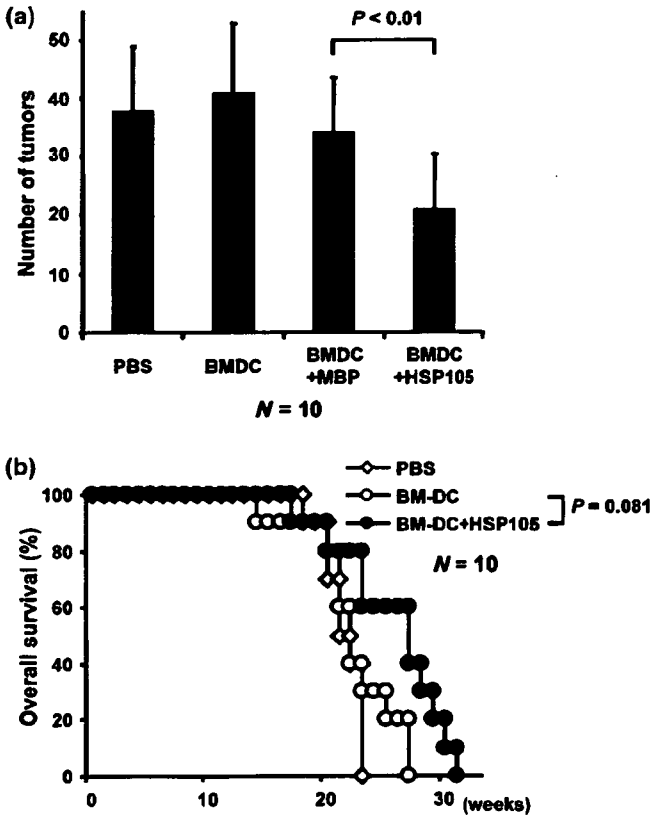

Fig. 2. Vaccination with heat shock protein (HSP) 105-pulsed bone marrow-derived dendritic cells (BM-DC) decreased the number of polyps in the small intestine of the $Apc^{Min/+}$ mice. (a) The $Apc^{Min/+}$ mice were inoculated intraperitoneally with HSP105-pulsed BM-DC (5×10^5), BM-DC alone, or myelin basic protein-pulsed BM-DC or phosphate-buffered saline (PBS) at 6, 8, and 10 weeks of age. At 12 weeks of age, the small intestines of the $Apc^{Min/+}$ mice were excised, stained with methylene blue, and the number of tumors was counted by the naked eye. Each group consisted of 10 $Apc^{Min/+}$ mice. The statistical significance of the differences in results was determined using an unpaired *t*-test. (b) The survival rate of $Apc^{Min/+}$ mice immunized with HSP105-pulsed BM-DC, BM-DC alone, or PBS as a control. The immunization protocol was the same as that of (a). The overall survival rate was calculated using the Kaplan–Meier method, and statistical significance was evaluated using Wilcoxon's test.

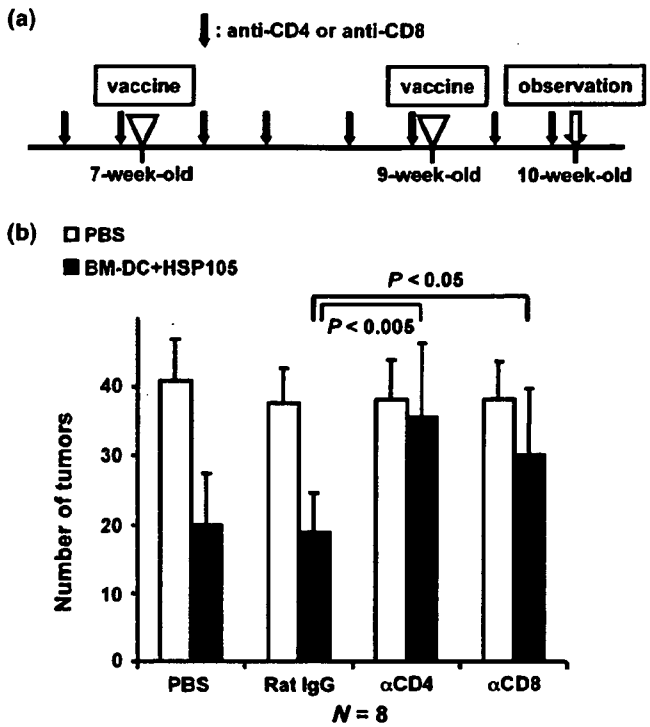

Fig. 3. Both $CD4^+$ and $CD8^+$ T cells are involved in the antitumor immunity elicited by the heat shock protein (HSP) 105-pulsed dendritic cell vaccine. (a) The protocol for the vaccination and the depletion of T cell subsets. (b) The number of polyps in the small intestine of $Apc^{Min/+}$ mice with various treatments. The number of tumors was counted as described in the legend for Fig. 2. Each group consisted of eight $Apc^{Min/+}$ mice. The statistical significance of the difference between the results was determined using the unpaired *t*-test.

the specific objective of the present study was to find out whether HSP105-pulsed DC-based immunotherapy can be used as a potent new strategy for the prevention of spontaneously arising tumors in FAP patients.

The ELISPOT assay shown in Figure 4a shows that both $CD4^+$ and $CD8^+$ HSP105-reactive T cells were primed in the mice immunized with HSP105-pulsed BM-DC. In this assay, we cannot completely rule out the possibility that responses were directed against contaminated bacteria-derived molecules in the HSP105 recombinant protein preparation. However, we consider this unlikely because practically no response was observed against BM-DC loaded with recombinant MBP protein, which was prepared from bacterial lysate in the same way as the preparation of recombinant HSP105. These recombinant proteins were purified extensively as described in a previous paper,[14] and contamination of lipopolysaccharide (LPS) or other DC-stimulants was ruled out.

Previous studies have reported that HSP105 is overexpressed specifically in a variety of human cancers and mouse tumor cells.[13,14] The present study demonstrated that HSP105 was also strongly expressed in the adenomatous polyps of $Apc^{Min/+}$ mice. In human tissue, the overexpression of HSP105 is a late event in the adenoma–carcinoma sequence, because immunohistochemical analysis revealed that HSP105 is strongly expressed in adenocarcinoma but not in adenoma.[13] Although the $Apc^{Min/+}$ mouse model has provided useful information about the pathogenesis of colorectal cancer, it is limited because it does not completely mimic the disease in humans. In humans, patients with FAP develop hundreds to thousands of adenomatous polyps, predominantly in the distal colon, and have a high risk of malignancies before the age of 40 years.[23] In contrast, $Apc^{Min/+}$ mice develop dozens to hundreds of adenomas and have a shortened life span. However, these adenomas are located mainly in the small intestine and they generally do not become malignant.[10] Furthermore, mice carrying different *Apc* mutations have been established. Tumors arising in these mice are histologically similar, but vary with respect to age of onset, number of tumors, and location.[24] Given this variation, the pattern of HSP105 expression in intestinal tumors may be different between human and $Apc^{Min/+}$ mice. Regardless of these differences, the $Apc^{Min/+}$ mice provide an appropriate model for analysis of the efficacy of the HSP105-pulsed BM-DC vaccine for inhibition of the development of human colorectal cancer, because the loss of *APC* function is the initiating event in not only FAP but also in the vast majority of sporadic colon cancers.

Recent findings regarding the cellular and molecular pathogenesis of colorectal cancer have led to the development of new targeted therapeutic options. Overexpression of COX-2 is one of the most significant observations in this respect.[25] The use of COX-2 inhibitor suppresses the development of colon cancer in

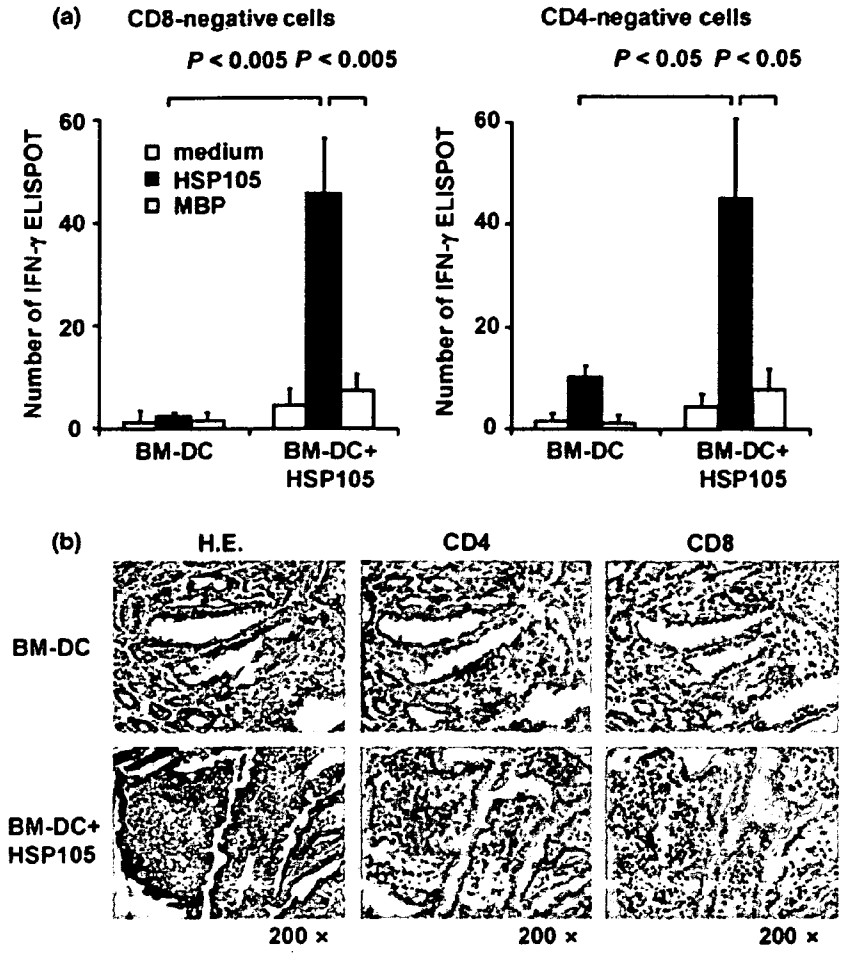

Fig. 4. Induction of heat shock protein (HSP) 105-specific T cells via immunization with HSP105-pulsed bone marrow-derived dendritic cells (BM-DC). (a) The $Apc^{Min/+}$ mice were inoculated with HSP105-pulsed BM-DC or BM-DC at 6 and 8 weeks of age. The spleen cells were harvested from 10-week-old $Apc^{Min/+}$ mice and depleted with either $CD4^+$ or $CD8^+$ cells using magnetic cell-sorting system. $CD4^-$ cells were used as a source of $CD8^+$ T cells and antigen-presenting cells, and $CD8^-$ cells were used as a source of $CD4^+$ T cells and antigen-presenting cells. Thereafter interferon-γ enzyme-linked immunospot (ELISPOT) assays were carried out. Briefly, $CD4^-$ or $CD8^-$ T cells (5×10^5) in each well were cultured together with 2 μg/mL HSP105, myelin basic protein, or medium alone for 24 h. The statistical significance of the difference in results was determined using the unpaired *t*-test. The spleens of three mice from each group were pooled. This experiment was carried out three times, with similar results. (b) The $Apc^{Min/+}$ mice were inoculated with HSP105-pulsed BM-DC or BM-DC at 6 and 8 weeks of age. The small intestines were excised from 10-week-old $Apc^{Min/+}$ mice and then were analyzed after immunohistochemical staining with anti-CD4 monoclonal antibody or anti-CD8 monoclonal antibody (magnification ×200).

sporadic cases[26] and FAP;[27] however, recent clinical trials suggest that the use of high doses of COX-2 inhibitor may have dangerous side-effects, such as increased risk of cardiovascular disease.[28] In the present study, no apparent autoimmunity was observed in the $Apc^{Min/+}$ mice immunized with HSP105-pulsed BM-DC, an observation similar to our previous findings.[14,22] In some human clinical trials of DC-based cancer immunotherapy, even in patients with advanced stages of cancer, no major toxicity nor severe side-effects were observed.[29–31] These results strongly suggest that DC-based immunotherapy is safe and feasible.

DC vaccination is now considered to be one of the most promising strategies for cancer immunotherapy.[32,33] DC are the most potent antigen-presenting cells and can present tumor antigens to stimulate a tumor-specific T-cell response. However, this does not occur in most types of cancer and in animal models of spontaneously arising tumors.[34] In the present study, immunization with HSP105-pulsed BM-DC vaccine significantly reduced the number of small-intestinal polyps in the $Apc^{Min/+}$ mice; however, the duration of survival was not prolonged as had been expected because the adenomas in $Apc^{Min/+}$ mice generally did not become malignant. Thereby, the protocol of DC-based vaccination used in the present study was not sufficient to completely prevent the occurrence of the tumors *in vivo*, and we are trying to establish a more effective immunization protocol. New strategies are now being developed to improve the clinical efficacy of DC-based vaccines, for example, the use of overexpression of Akt1 in BM-DC, suppressor of cytokine signaling 1-silenced BM-DC, and CD40-inducible DC.[35–37] The use of transfected DC in a protocol such as that used in the present study has the potential to induce a more effective antitumor response. Furthermore, it is necessary to investigate whether combinations of immunotherapy and other therapies, such as combinations of DC vaccines and chemotherapy or low-dose COX-2 inhibitors, induce a more effective antitumor response in comparison to individual therapy alone, thereby developing more effective strategies for treating colorectal cancer. Recent findings have shown the curative potential of combinations of irradiation,[38] chemotherapy,[39] and subsequent adoptive T-cell immunotherapy against established solid tumors.[40]

The abrogation of the antitumor effect of the HSP105-pulsed BM-DC vaccine, after the depletion of $CD4^+$ cells or $CD8^+$ cells via the administration of mAb, indicates that both $CD4^+$ and $CD8^+$ T cells play a critical role in the antitumor effect of HSP105-pulsed BM-DC. The report that antigen-specific $CD4^+$ T helper cells are required for the activation of $CD8^+$ effector T cells, their secondary expansion, and memory induction,[41] is consistent with the findings that $CD4^+$ T cells played an important role in tumor rejection in the present study. Peptides derived from HSP105 incorporated into BM-DC might be presented in the context of MHC class II on the surface of BM-DC to activate $CD4^+$ T cells. Subsequently, $CD4^+$ T cells produce interferon-γ and interleukin-2 to activate HSP105-specific $CD8^+$ effector T cells and facilitate the development of HSP105-specific $CD8^+$ memory T cells. Furthermore, the ELISPOT assay showed that HSP105-specific $CD8^+$ T cells were also activated by HSP105-pulsed antigen-presenting cells. These results indicate

doi: 10.1111/j.1349-7006.2007.00612.x

that HSP105-pulsed BM-DC can demonstrate peptides derived from exogenously added HSP105 not only in the context of MHC class II molecules to activate CD4+ T cells but also in the context of MHC class I molecules via the mechanism of cross-presentation to activate CD8+ T cells. Whole-protein-pulsed DC vaccines seem to be superior to peptide-pulsed DC because they can activate both CD4+ and CD8+ T cells, and it does not require a knowledge of the human leukocyte antigen (HLA) type of the cancer patients.

In conclusion, the results of the present study indicate that HSP105-pulsed BM-DC may provide a potential vaccine to combat human colorectal cancer. It is possible that immunization with HSP105-pulsed BM-DC vaccines could be useful in patients with colorectal cancer to prevent tumor recurrence after surgical resection. Although there was a noteworthy effect of this type of vaccine on the host immune response to tumors expressing HSP105, further investigation to improve the clinical efficacy of HSP105-pulsed BM-DC vaccines is called for.

Acknowledgments

This work was supported in part by Grants-in-Aid (no. 12213111 for Y. Nishimura, no. 14770142 for T. Nakatsura, and no. 14770142 for S. Senju) from the Ministry of Education, Science, Technology, Sports, and Culture, Japan, and The Sagawa Foundation for Promotion of Cancer Research and Meiji Institute of Health Science.

References

1 Weitz J, Koch M, Debus J, Hohler T, Galle PR, Büchler MW. Colorectal cancer. *Lancet* 2005; **365**: 153–65.
2 Tournigand C, André T, Achille E *et al.* FOLFIRI followed by FOLFOX6 or the reverse sequence in advanced colorectal cancer: a randomized GERCOR study. *J Clin Oncol* 2004; **22**: 229–37.
3 Rao CV, Cooma I, Rosa Rodriguez JG, Simi B, El-Bayoumy K, Reddy BS. Chemoprevention of familial adenomatous polyposis development in the *Apc*^{Min} mouse model by 1,4-phenylene *bis*(methylene)selenocyanate. *Carcinogenesis* 2000; **21**: 617–21.
4 Kinzler KW, Vogelstein B. Cancer-susceptibility genes: gatekeepers and caretakers. *Nature* 1997; **386**: 761–3.
5 Fearon ER, Vogelstein B. A genetic model for colorectal tumorigenesis. *Cell* 1990; **61**: 759–67.
6 Kikuchi A. Modulation of Wnt signaling by Axin and Axil. *Cytokine Growth Factor Rev* 1999; **10**: 255–65.
7 Sancho E, Batlle E, Clevers H. Signaling pathways in intestinal development and cancer. *Annu Rev Cell Dev Biol* 2004; **20**: 695–723.
8 Miyoshi Y, Ando H, Nagase H *et al.* Germ-line mutations of the *APC* gene in 53 familial adenomatous polyposis patients. *Proc Natl Acad Sci USA* 1992; **89**: 4452–6.
9 Su LK, Kinzler KW, Vogelstein B *et al.* Multiple intestinal neoplasia caused by a mutation in the murine homolog of the *APC* gene. *Science* 1992; **256**: 668–70.
10 Moser AR, Pitot HC, Dove WF. A dominant mutation that predisposes to multiple intestinal neoplasia in the mouse. *Science* 1990; **247**: 322–4.
11 Feder ME, Hofmann GE. Heat-shock proteins, molecular chaperones, and the stress response: evolutionary and ecological physiology. *Annu Rev Physiol* 1999; **61**: 243–82.
12 Nakatsura T, Senju S, Yamada K, Jotsuka T, Ogawa M, Nishimura Y. Gene cloning of immunogenic antigens overexpressed in pancreatic cancer. *Biochem Biophys Res Commun* 2001; **281**: 936–44.
13 Kai M, Nakatsura T, Egami H, Senju S, Nishimura Y, Ogawa M. Heat shock protein 105 is overexpressed in a variety of human tumors. *Oncol Rep* 2003; **10**: 1777–82.
14 Yokomine K, Nakatsura T, Minohara M *et al.* Immunization with heat shock protein 105-pulsed dendritic cells leads to tumor rejection in mice. *Biochem Biophys Res Commun* 2006; **343**: 269–78.
15 Miyazaki M, Nakatsura T, Yokomine K *et al.* DNA vaccination of HSP105 leads to tumor rejection of colorectal cancer and melanoma in mice through activation of both CD4+ T cells and CD8+ T cells. *Cancer Sci* 2005; **96**: 695–705.
16 Hosaka S, Nakatsura T, Tsukamoto H, Hatayama T, Baba H, Nishimura Y. Synthetic small interfering RNA targeting heat shock protein 105 induces apoptosis of various cancer cells both *in vitro* and *in vivo*. *Cancer Sci* 2006; **97**: 623–32.
17 Srivastava P. Interaction of heat shock proteins with peptides and antigen presenting cells: chaperoning of the innate and adaptive immune responses. *Annu Rev Immunol* 2002; **20**: 395–425.
18 Manjili MH, Wang XY, Chen X *et al.* HSP110-HER2/neu chaperone complex vaccine induces protective immunity against spontaneous mammary tumors in HER-2/neu transgenic mice. *J Immunol* 2003; **171**: 4054–61.
19 Wang XY, Chen X, Manjili MH, Repasky E, Henderson R, Subjeck JR. Targeted immunotherapy using reconstituted chaperone complexes of heat shock protein 110 and melanoma-associated antigen gp100. *Cancer Res* 2003; **63**: 2553–60.
20 Dietrich WF, Lander ES, Smith JS *et al.* Genetic identification of *Mom*-1, a major modifier locus affecting *Min*-induced intestinal neoplasia in the mouse. *Cell* 1993; **75**: 631–9.
21 Yamagishi N, Nishihori H, Ishihara K, Ohtsuka K, Hatayama T. Modulation of the chaperone activities of Hsc70/Hsp40 by Hsp105α and Hsp105β. *Biochem Biophys Res Commun* 2000; **272**: 850–5.
22 Nakatsura T, Komori H, Kubo T *et al.* Mouse homologue of a novel human oncofetal antigen, glypican-3, evokes T-cell-mediated tumor rejection without autoimmune reaction in mice. *Clin Cancer Res* 2004; **10**: 8630–40.
23 Fearnhead NS, Wilding JL, Bodmer WF. Genetics of colorectal cancer: hereditary aspects and overview of colorectal tumorigenesis. *Br Med Bull* 2002; **64**: 27–43.
24 Boivin GP, Washington K, Yang K *et al.* Pathology of mouse models of intestinal cancer: consensus report and recommendations. *Gastroenterology* 2003; **124**: 762–77.
25 Oshima M, Dinchuk JE, Kargman SL *et al.* Suppression of intestinal polyposis in *Apc* Δ716 knockout mice by inhibition of cyclooxygenase 2 (COX-2). *Cell* 1996; **87**: 803–9.
26 Reddy BS, Hirose Y, Lubet R *et al.* Chemoprevention of colon cancer by specific cyclooxygenase-2 inhibitor, celecoxib, administered during different stages of carcinogenesis. *Cancer Res* 2000; **60**: 293–7.
27 Steinbach G, Lynch PM, Philips RKS *et al.* The effect of celecoxib, a cyclooxygenase-2 inhibitor, in familial adenomatous polyposis. *N Engl J Med* 2000; **342**: 1946–52.
28 Solomon SD, McMurray JJV, Pfeffer MA *et al.* Cardiovascular risk associated with celecoxib in a clinical trial for colorectal adenoma prevention. *N Engl J Med* 2005; **352**: 1071–80.
29 Nestle FO, Alijagic S, Gilliet M *et al.* Vaccination of melanoma patients with peptide- or tumor lysate-pulsed dendritic cells. *Nat Med* 1998; **4**: 328–32.
30 Stift A, Friedl J, Dubsky P *et al.* Dendritic cell-based vaccination in solid cancer. *J Clin Oncol* 2003; **21**: 135–42.
31 Yu JS, Liu G, Ying H, Yong WH, Black KL, Wheeler CJ. Vaccination with tumor lysate-pulsed dendritic cells elicits antigen-specific, cytotoxic T-cells in patients with malignant glioma. *Cancer Res* 2004; **64**: 4973–9.
32 Timmerman JM, Levy R. Dendritic cell vaccines for cancer immunotherapy. *Annu Rev Med* 1999; **50**: 507–29.
33 Fong L, Engleman EG. Dendritic cells in cancer immunotherapy. *Annu Rev Immunol* 2000; **18**: 245–73.
34 Gabrilovich D. Mechanisms and functional significance of tumour-induced dendritic-cell defects. *Nature Rev Immunol* 2004; **4**: 941–52.
35 Park D, Lapteva N, Seethammagari M, Slawin KM, Spencer D. An essential role for Akt1 in dendritic cell function and tumor immunotherapy. *Nat Biotechnol* 2006; **24**: 1581–90.
36 Evel-Kabler K, Song XT, Aldrich M, Huang XF, Chen SY. SOCS1 restricts dendritic cells' ability to break self tolerance and induce antitumor immunity by regulating IL-12 production and signaling. *J Clin Invest* 2006; **116**: 90–100.
37 Hanks BA, Jiang J, Singh RAK *et al.* Re-engineered CD40 receptor enables potent pharmacological activation of dendritic-cell cancer vaccines *in vivo*. *Nat Med* 2005; **11**: 130–7.
38 Reits EA, Hodge JW, Herberts CA *et al.* Radiation modulates the peptide repertoire, enhances MHC class I expression, and induces successful antitumor immunotherapy. *J Exp Med* 2006; **203**: 1259–71.
39 Casares N, Pequignot MO, Tesniere A *et al.* Caspase-dependent immnogenicity of doxorubicin-induced tumor cell death. *J Exp Med* 2005; **202**: 1691–701.
40 Zhang B, Bowerman NA, Salama JK *et al.* Induced sensitization of tumor stroma leads to eradication of established cancer by T cells. *J Exp Med* 2007; **204**: 49–55.
41 Janssen EE, Lemmens EE, Wolfe T, Christen U, von Herrath MG, Schoenberger SP. CD4+ T cells are required for secondary expansion and memory in CD8+ T lymphocytes. *Nature* 2003; **421**: 852–6.

Hyperglycemia During the Neutropenic Period Is Associated With a Poor Outcome in Patients Undergoing Myeloablative Allogeneic Hematopoietic Stem Cell Transplantation

Shigeo Fuji,[1] Sung-Won Kim,[1] Shin-ichiro Mori,[1] Takahiro Fukuda,[1] Shigemi Kamiya,[2] Satoshi Yamasaki,[1] Yuriko Morita-Hoshi,[1] Fusako Ohara-Waki,[1] Osamu Honda,[3] Setsuko Kuwahara,[2] Ryuji Tanosaki,[1] Yuji Heike,[1] Kensei Tobinai,[1] and Yoichi Takaue[1,4]

Background. Recipients of allogeneic hematopoietic stem cell transplantation (HSCT) frequently require support with parenteral nutrition and immunosuppressive drugs, which introduce the risk of hyperglycemia. Van den Berghe et al. showed that the strict glucose control improved the outcome of patients treated in the intensive care unit, and this point was evaluated in this study in a HSCT setting.

Methods. A cohort of 112 consecutive adult patients treated by myeloablative allogeneic HSCT between January 2002 and June 2006 was reviewed retrospectively. Twenty-one patients were excluded due to graft failure, preexisting infectious diseases, preexisting neutropenia or previous allogeneic HSCT. The remaining 91 patients were categorized according to mean fasting blood glucose (BG) level in the neutropenic period after conditioning: normoglycemia (BG <110 mg/dL, n=28), mild hyperglycemia (110 to 150 mg/dL, n=49), and moderate/severe (>150 mg/dL, n=14). The primary endpoint was the occurrence of febrile neutropenia (FN) and documented infection during neutropenia, and the secondary endpoints included organ dysfunction according to the definition used by van den Berghe, acute graft-versus-host disease (GVHD), overall survival, and nonrelapse mortality (NRM).

Results. Although the incidence of FN or documented infections was similar between the three groups, hyperglycemia was significantly associated with an increased risk of organ dysfunction, grade II–IV acute GVHD, and NRM.

Conclusions. While the results suggested an association between the degree of hyperglycemia during neutropenia and an increased risk of posttransplant complications and NRM, the possibility that intensive glucose control improves the outcome after HSCT can only be confirmed in a prospective randomized trial.

Keywords: Allogeneic transplantation, Hyperglycemia, Nonrelapse mortality, Acute graft-versus-host disease.

(*Transplantation* 2007;84: 814–820)

Van den Berghe et al. showed with patients nursed in the intensive care unit (ICU) that the rigid control of hyperglycemia with intensive insulin therapy to keep the blood glucose level at 80–110 mg/dL reduced morbidity, including infections, and mortality compared to patients who received standard care maneuvers that maintained the level at <200 mg/dL (*1–3*). Although these results have been confirmed in several subsequent studies (*4–7*), the precise mechanism that underlies this association is unclear. In animal models, it has been shown that insulin itself has a direct inhibitory effect on the inflammation process (*8, 9*). However in human studies, it has been suggested that these benefits could be directly attributed to intense glucose control rather than to any pharmacological activity of administered insulin per se (*3, 4*).

Recipients of allogeneic hematopoietic stem cell transplantation (HSCT) suffer from serious complications including infection, graft-versus-host disease (GVHD) and organ dysfunction. They are also at higher risk of hyperglycemia due to the use of steroids for the treatment of graft-versus-host disease (GVHD), prolonged total parenteral nutrition (TPN), immunosuppressive drugs, and infectious complications (*10, 11*). This makes them susceptible to numerous serious complications, including multiple organ failure (*12–14*). In this study, we evaluated whether hyperglycemia during the cytopenic pe-

Supported in part by grants from the Ministry of Health, Labor and Welfare, Japan.

This paper was presented in part as a poster presentation at the tandem Meeting of ASBMT and IBMTR, Keystone, Colorado, February 2007.

[1] Department of Hematology and Stem Cell Transplantation, National Cancer Center Hospital, Tokyo, Japan.

[2] Division of Nutritional Management, National Cancer Center Hospital, Tokyo, Japan.

[3] Tokyo Anesthesiology Group, Tokyo, Japan.

[4] Address correspondence to: Yoichi Takaue, M.D., Department of Hematology, National Cancer Center Hospital., 5-1-1, Tsukiji, Chuo-Ku, Tokyo 104-0045, Japan.

E-mail: ytakaue@ncc.go.jp

Received 12 June 2007. Revision requested 10 July 2007.

Accepted 18 July 2007.

ISSN 0041-1337/07/8407-814

DOI: 10.1097/01.tp.0000282790.66889.a5

riod after conditioning for HSCT could be a significant risk factor for the subsequent clinical course.

PATIENTS AND METHODS

Patient Characteristics

A cohort of 112 consecutive adult patients who received myeloablative allogeneic HSCT between January 2002 and June 2006 at the National Cancer Center Hospital (Tokyo, Japan) was reviewed retrospectively. Twenty-one patients were excluded due to graft failure, pre-existing infectious diseases or neutropenia before HSCT, and previous allogeneic HSCT. The remaining 91 patients were subjected to further analysis, and their characteristics are listed in Table 1. Their median age was 36 years (range, 18–57 years), and their diagnosis included acute myeloid leukemia (AML, n=41), acute lymphoblastic leukemia (ALL, n=21), non-Hodgkin lymphoma (NHL, n=13), myelodysplastic syndrome (MDS, n=10), and chronic myelogenous leukemia (n=6). Standard-risk patients included those with acute leukemia in first complete remission, chronic leukemia in first chronic phase, MDS in refractory anemia, and NHL in complete remission, and the remaining patients were categorized as high-risk. Forty-six and 45 patients received a graft from a related donor and an unrelated donor, respectively. Stem cell sources included bone marrow (n=46), peripheral blood (n=41), and cord blood cells (n=4). In this study, only two patients were diagnosed as type 2 diabetes mellitus before HSCT, which reflects the low prevalence of this condition in Japan, especially in younger patients who can be the target of allogeneic HSCT with a myeloablative conditioning regimen. These two diabetic patients were included in the moderate and severe hyperglycemia group. None of the patients, including these two patients, had major organ dysfunction or diabetic complications before HSCT. For the transplantation procedure, signed informed consent was obtained according to the Declaration of Helsinki.

Transplantation Procedures

All patients received a myeloablative conditioning regimen that included oral busulfan (BU) plus cyclophosphamide (CY, n=45), CY plus 12 Gy total body irradiation (TBI, n=43) or cytarabine (CA) plus CY plus TBI (n=3: Table 1). GVHD prophylaxis included cyclosporine- (n=62) and tacrolimus-based regimens (n=29), with an additional short course of methotrexate (MTX) in 89 patients. Granulocyte

TABLE 1. Patient characteristics

Variable	Normoglycemia (<110 mg/dl)	Mild hyperglycemia (110–150 mg/dl)	Moderate and severe hyperglycemia (>150 mg/dl)
N	28	49	14
Blood glucose, median mg/dl (range)	104 (81–109)	120 (110–150)	168 (150–211)
Age, median years (range)	31 (21–52)	36 (18–57)	45 (30–57)
<40	20 (71)	32 (65)	4 (29)
≥40	8 (29)	17 (35)	10 (71)
Sex			
Male	9 (32)	34 (69)	8 (57)
Female	19 (68)	15 (31)	6 (43)
Disease risk			
Standard	16 (57)	18 (37)	6 (43)
High	12 (43)	31 (63)	8 (57)
Conditioning			
TBI-containing	11 (39)	26 (53)	9 (64)
Non-TBI-containing	17 (61)	23 (47)	5 (36)
GVHD prophylaxis			
Cyclosporine-based	24 (86)	33 (67)	5 (36)
Tacrolimus-based	4 (14)	16 (33)	9 (74)
Relation to donor			
Related	19 (68)	24 (49)	3 (21)
Unrelated	9 (32)	25 (51)	11 (79)
Stem cell source			
Bone marrow	11 (39)	24 (49)	11 (79)
PBSC	16 (57)	22 (45)	3 (21)
Cord blood	1 (4)	3 (6)	0 (0)
HLA match			
Match	25 (89)	34 (69)	10 (71)
Mismatch	3 (11)	15 (31)	4 (29)

Data are n (%) unless noted.
TBI, total body irradiation; GVHD, graft-versus-host disease; PBSC, peripheral blood stem cells; HLA, human leukocyte antigen.

colony-stimulating factor (G-CSF) was administered in all patients from day +6 after transplantation until engraftment. Most patients received ciprofloxacin (200 mg orally three times daily) for bacterial prophylaxis until neutrophil engraftment. Fluconazole (100 mg once daily) was administered for fungal prophylaxis. Low-dose acyclovir was given for prophylaxis against herpes simplex virus and varicella zoster virus until the cessation of immunosuppressive agents. Prophylaxis against *Pneumocystis jiroveci* infection consisted of trimethoprim-sulfamethoxazole (400 mg of sulfamethoxazole once daily) from the first day of conditioning to day −3 of transplantation, and from day +28 until day +180 or the cessation of immunosuppressive agents. Patients who developed fever during the neutropenic period were treated with cefepime, and additional agents including vancomycin, aminoglycosides and amphotericin B were given as clinically indicated. Neutrophil engraftment was defined as the first of 3 consecutive days after transplantation that the absolute neutrophil count exceeded 0.5×10^9/L.

Grouping of Patients

Patients were categorized according to the mean blood glucose (BG) level in the preengraftment neutropenic period: normoglycemia BG maintained at <110 mg/dL (group 1, n=28), mild hyperglycemia at 110–150 mg/dL (group 2, n=49), and moderate/severe hyperglycemia at >150 mg/dL (group 3, n=14). Blood glucose level was routinely tested in the morning at least three times a week. Daily caloric intake was calculated by dietitian following the chart record.

Outcome Measures

The primary outcome measure was the occurrence of febrile neutropenia (FN) and documented infection including bacteremia, pneumonia and central venous catheter infection in the neutropenic period. Secondary outcome measurements were organ dysfunction in the neutropenic period, acute GVHD, overall survival (OS) and nonrelapse mortality (NRM). Organ dysfunction was defined with reference to van den Berghe (*5–7*) as follows: 1) hypercreatininemia: serum creatinine level ≥2.0 mg/dL or more than twice the baseline; 2) hyperbilirubinemia: serum total bilirubin level ≥2.0 mg/dL; and 3) increased inflammatory markers: serum C-reactive protein (CRP) level ≥15 mg/dL. Acute GVHD was graded by the Consensus Criteria (*15*).

Statistical Analyses

Standard descriptive statistics were used. The Student's *t*-test, chi-square, and Wilcoxon rank-sum tests were used to compare clinical and patient characteristics. Multiple logistic regression analysis was conducted to ascertain odds ratios (ORs) and 95% confidence intervals (CIs). OS was estimated using Kaplan-Meier curves. The cumulative incidences of NRM were estimated based on a Cox regression model for the cause-specific hazards by treating progressive disease or relapse as a competing event. Cox proportional hazard models were used for multivariate analysis of variables on NRM and OS after HCT. Clinical factors that were assessed for their association with NRM and OS included patient age, sex, conditioning regimen (TBI-based vs. non-TBI-based), donor [human leukocyte antigen (HLA)-matched vs. HLA-mismatched, related vs. unrelated], GVHD prophylaxis (cyclosporine-based vs. tacrolimus-based) and disease risk (standard vs. high). Factors with $P<0.10$ in the univariate analyses were subjected to a multivariate analysis. A level of $P<0.05$ was defined as statistically significant. All P values are two-sided. All analyses were performed using SPSS 10.0 statistical software (Chicago, IL).

RESULTS

Patients and Transplantation Characteristics

The median ages of the patients in the normoglycemia, mild hyperglycemia, and moderate/severe hyperglycemia groups were, respectively, 31, 36, and 45 years. The percentages of patients who received graft from an unrelated donor were 32%, 51%, and 79%, and the percentages of patients who received GVHD prophylaxis with tacrolimus were 14%, 33%, and 74%. To clarify the risk factor to be included in moderate and severe hyperglycemia group, logistic analysis was performed, which showed older age and GVHD prophylaxis with tacrolimus were associated with moderate and severe hyperglycemia [$P=0.04$, OR 3.9 (1.1–14.0), and $P=0.01$, OR 5.5 (1.5–20.3), respectively], and there was a trend that patients who received stem cell from unrelated donor were associated with moderate and severe hyperglycemia [$P=0.07$, OR 3.6 (0.9–14.2)]. Multiple logistic analysis showed age more than 40 years old and GVHD prophylaxis with tacrolimus were associated with moderate and severe hyperglycemia [$P=0.042$, OR 4.1 (1.1–15.7), and $P=0.01$, OR 5.8 (1.5–22.1), respectively].

Although in practice we generally keep the parenteral glucose dose relatively low to avoid severe metabolic complications including hyperglycemia and hyperlipidemia during the acute phase of allogeneic HSCT, the possibility that the dose of parenteral nutrition affects the blood glucose level should be explored. We calculated the total caloric intake by combining both oral and parenteral nutrition. Although the mild hyperglycemia group received significantly more parenteral nutrition than the normoglycemia group (group 1 694+322 kcal/day vs. group 2 969+383 kcal/day), overall there was no essential difference in caloric intake between the three groups (1070+303 kcal/day, 1190+393 kcal/day, 1045+530 kcal/day, respectively). The median duration of the follow-up time in surviving patients was 809 days (range, 132-1530 days) in group 1, 369 days (105–1550 days) in group 2, and 587 days (170–774 days) in group 3. Described as hydrocortisone-equivalent dose, the median dose of corticosteroid used during neutropenia was 0 mg (0–1610 mg) in group 1, 100 mg (0–9700 mg) in group 2, and 375 mg (0–2468 mg) in group 3. Statistically more dose of corticosteroid was used in group 2 and group 3, compared with group 1.

Primary Endpoints

The incidence of FN and documented infections is summarized in Table 2. The incidences of FN and documented infections including bacteremia, pneumonia, and central venous catheter infection in groups 1, 2 and 3 were, respectively, 89% and 32% (25%, 4% and 11%), 88% and 20% (16%, 6% and 6%), and 98% and 43% (36%, 14% and 14%). Overall, no statistically significant difference was observed between the three groups in the incidence of infectious episodes, including FN and documented infections.

TABLE 2. Endpoints

Variable	Normoglycemia (<110 mg/dl)	Mild hyperglycemia (110–150 mg/dl)	Moderate and severe hyperglycemia (>150 mg/dl)
N	28	49	14
Febrile neutropenia	23 (89)	43 (88)	13 (98)
Documented infection	9 (32)	10 (20)	6 (43)
Bacteremia	7 (25)	8 (16)	5 (36)
Pneumonia	1 (4)	3 (6)	2 (14)
Central-venous catheter infection	3 (11)	3 (6)	2 (14)
Organ dysfunction			
Hypercreatininemia	1 (4)	4 (8)	4 (29)
Hyperbilirubinemia	3 (11)	11 (22)	6 (43)
Increased inflammatory markers	4 (14)	15 (31)	9 (64)

Data are n (%).

Hypercreatininemia, serum creatinine level ≥2.0 mg/dl or more than twice of baseline; hyperbilirubinemia, serum bilirubin level ≥2.0 mg/dl; increased inflammatory markers, serum C-reactive protein level ≥15 mg/dl.

Secondary Endpoints

The incidence of hypercreatininemia was 4% in group 1, 8% in group 2 and 29% in group 3, as summarized in Table 2, and that in group 3 was significantly higher than those in group 1 (OR 10.8, 95% CI 1.1–108.6; $P=0.018$) and group 2 (OR 4.5, 95% CI 1.0–21.1; $P=0.043$). The incidence of hyperbilirubinemia was, respectively, 11%, 22% and 43%, in the three groups, and that in group 3 was significantly higher than that in group 1 (OR 6.3, 95% CI 1.3–30.9; $P=0.017$). The incidence of increased inflammatory markers was, respectively, 14%, 31% and 64%, and that in group 3 was significantly higher than those in group 1 (OR 10.8, 95% CI 2.4–49.5; $P<0.001$) and group 2 (OR 4.1, 95% CI 1.2–14.3; $P=0.022$). Multiple logistic regression analysis showed that the degree of hyperglycemia was associated with hypercreatininemia, hyperbilirubinemia, and increased inflammatory markers (Table 3).

TABLE 3. Multiple logistic regression analysis for organ dysfunction and multiple variate analysis for acute GVHD, nonrelapse mortality, and overall survival

Outcomes and variables	Odds/hazard ratio	95% CI	*P* value
Multiple logistic regression analysis			
Hypercreatininemia			
Hyperglycemia	5.2	1.1–24.6	0.039
Hyperbilirubinemia			
Hyperglycemia	4.9	1.6–14.9	0.005
Increased inflammatory markers			
Hyperglycemia	6.7	2.2–20.3	0.001
Tacrolimus-based	6.9	1.6–30.5	0.011
Multivariate analysis (Cox-proportional hazard model)			
Acute GVHD			
Hyperglycemia	2.3	1.2–4.3	0.013
Disease risk (high)	2.3	1.0–5.1	0.047
HLA mismatch	2.8	1.3–5.9	0.009
Nonrelapse mortality			
Hyperglycemia	2.9	1.2–6.6	0.013
Disease risk (high)	2.7	0.9–8.7	0.091
Overall survival			
Hyperglycemia	2.0	1.1–3.6	0.019
TBI-containing	2.3	1.1–5.0	0.035
Disease risk (high)	1.9	0.9–4.1	0.10

Odds ratios are presented for multiple logistic regression analysis; hazard ratios are presented for multivariate analysis.

GVHD, graft versus host disease; TBI, total body irradiation.

The cumulative incidence of grade II–IV acute GVHD is shown in Figure 1. The degree of hyperglycemia was associated with a higher incidence of grade II–IV acute GVHD

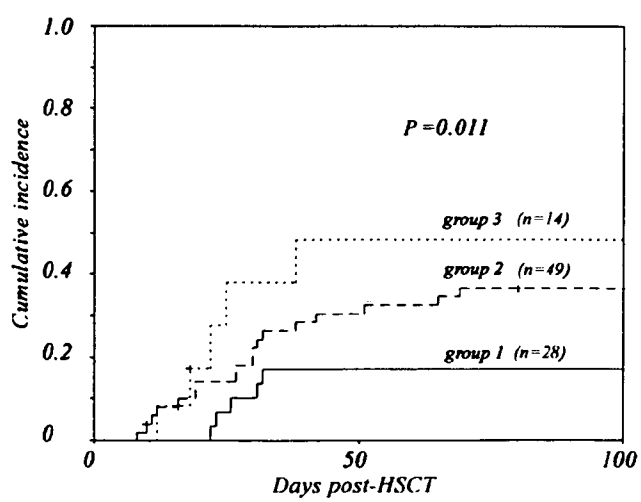

FIGURE 1. Cumulative incidence of acute GVHD grade II–IV stratified according to the mean glucose level during neutropenia. Group 1 included patients with normoglycemia, group 2 included patients with mild hyperglycemia, and group 3 included patients with moderate and severe hyperglycemia.

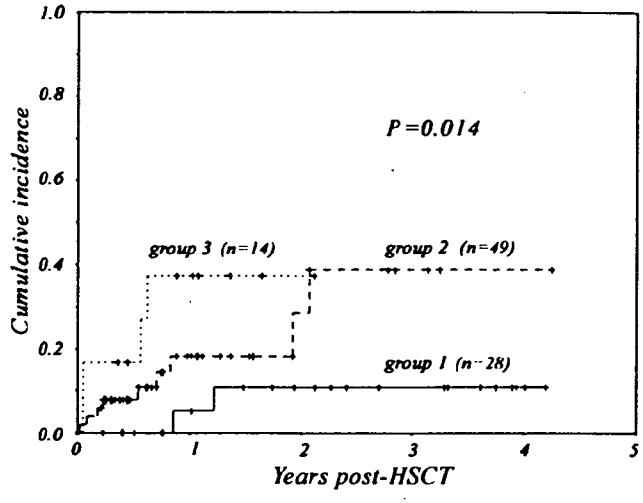

FIGURE 2. Cumulative incidence of treatment-related mortality stratified according to the mean glucose level during neutropenia.

(P=0.002). A Cox proportional hazard model showed that hyperglycemia, high-risk underlying disease, and HLA mismatch were risk factors for grade II-IV acute GVHD (Table 3).

The cumulative incidence of NRM was, respectively, 5%, 17%, and 35% at 1 year, and was significantly related to the degree of hyperglycemia (P=0.014; Fig. 2). The probability of OS was, respectively, 88%, 70%, and 56%, and was significantly associated with hyperglycemia (P=0.008; Fig. 3). A Cox proportional hazard model showed that the degree of hyperglycemia was associated with NRM and OS (Table 3).

DISCUSSION

In this study, we evaluated whether hyperglycemia during the cytopenic period after conditioning for HSCT could be a significant risk factor for the subsequent clinical course. Infectious diseases remain a major cause of morbidity and mortality in patients who receive HSCT, and we speculated that this might be exaggerated in the presence of hyperglycemia. Alternatively, hyperglycemia can be caused by infectious diseases and also aggravates infectious diseases to lead to a vicious cycle, with resultant morbidities that include organ dysfunction and mortality. Theoretically, strict glucose control should prevent this vicious cycle and help to reduce morbidity and mortality in patients after HSCT, as shown previously in ICU settings (*1*, *2*). However, in this study the incidences of FN and documented infections were not different among the three groups. On the other hand, we found that hyperglycemia was associated with organ dysfunction and increased inflammatory markers, which was consistent with previous reports that demonstrated the impact of hyperglycemia on clinical outcomes of patients suffering from nonhematological diseases (*1–3*, *12–14*). Additionally, a multivariate analysis showed that hyperglycemia was a risk factor for acute GVHD.

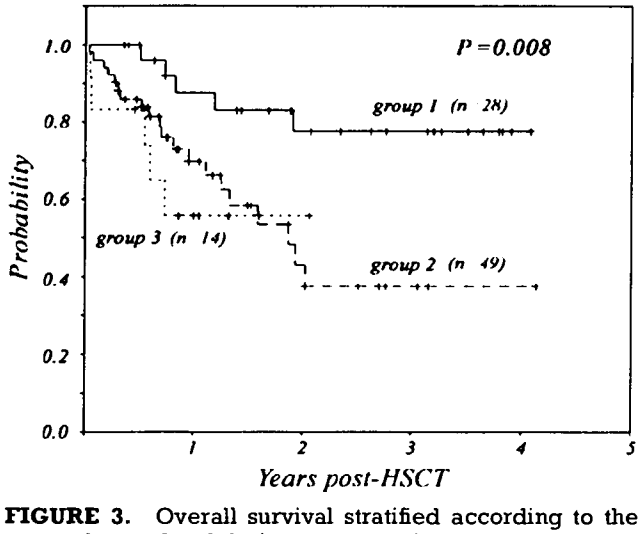

FIGURE 3. Overall survival stratified according to the mean glucose level during neutropenia.

The reason for the association between early hyperglycemia and late complications needs to be clarified. The increase in the levels of circulating cytokines due to hyperglycemia may further aggravate hyperglycemia itself (*16–21*). Therefore, this condition which occurs during the critical period of neutropenia before engraftment may influence the afferent phase of acute GVHD, as suggested by Ferrara et al. Elevated cytokine levels during the afferent phase then lead to subsequent acute GVHD in the effector phase (*22*, *23*). Teshima et al. reported that the effector phase of acute GVHD is not antigen-specific and inflammatory cytokines mediate target destruction (*24*), and other reports have shown that inflammatory cytokines were required in acute GVHD and these molecules can cause tissue damage (*25–27*). With these reports in mind, it is reasonable to speculate that the aggravated production of inflammatory cytokines by hyperglycemia may be a risk factor in the pathogenesis of acute GVHD and organ dysfunction.

This study has several limitations, including heterogeneous patient populations and a retrospective nature. First, hyperglycemia can be caused by infection itself and it has been previously shown that the level of hyperglycemia was correlated with the severity of illness (*4*). In this retrospective study, we could not confirm whether hyperglycemia directly influenced organ dysfunction or increased inflammatory markers. Furthermore, statistically more corticosteroid was used in the group of moderate and severe hyperglycemia, and statistically more parenteral nutrition was used in the group of mild hyperglycemia. However, the observation that hyperglycemia and the severity of illness were independently associated with a worse prognosis has been well confirmed in the ICU setting (*4*), and several prospective studies have shown that intensive glucose control reduced both morbidity and mortality (*1*, *2*). Considering these findings, we suggest that our data still support the possibility that the degree of hyperglycemia was associated with morbidity and mortality in the allogeneic HSCT setting. Second, we must consider that the patients who developed moderate and severe hyperglycemia included older patients, those who received more unrelated grafts, and those who received tacrolimus compared to other groups. In terms of immunosuppressive drugs, tacrolimus has recently become a preferred immunosuppressive drug for GVHD prophylaxis in unrelated or HLA-mismatched HSCT, based on the results of two Japanese studies, which showed that, compared to cyclosporine, tacrolimus was associated with a lower incidence of acute GVHD and better overall survival, which were similar to those in related HSCT, even

after HSCT with alternative donors, including unrelated donors (*28, 29*). Therefore, the effect of unrelated graft and tacrolimus on the incidence of acute GVHD and NRM might not be significant in this study.

The effects of tacrolimus on hyperglycemia, hyperbilirubinemia, and hypercreatininemia need to be clarified. It is well known that hyperglycemia occurs more often in patients receiving tacrolimus than in those receiving cyclosporine (*30–32*). In the present study, patients receiving tacrolimus were more likely to have moderate to severe hyperglycemia. However, the association of hyperbilirubinemia with tacrolimus has not been previously reported and two other studies (*33, 34*) showed that cyclosporine was more likely to cause hyperbilirubinemia than tacrolimus after allogeneic HSCT or kidney transplantation. Although the relative nephrotoxicity attributed to tacrolimus compared to cyclosporine has been controversial (*30, 33, 35*), studies that have reported such nephrotoxicity used a higher target tacrolimus level (>20 ng/ml) (*30, 35*). On the other hand, it has been reported that the use of lower levels of tacrolimus (10–15 ng/ml in our hospital) was associated with reduced complications in allogeneic HSCT (*36, 37*), with no difference in the incidence of hypercreatininemia compared to cyclosporine (*33*). Based on a consideration of all of these results, we think that tacrolimus might not be the direct cause of hypercreatininemia in this study. Finally, due to the nature of this retrospective study, during the period evaluated we did not apply any consistent protocol for glucose control and nutritional support, although we tried to avoid severe hyperglycemia (BG ≥200 mg/dl), which certainly biases the interpretation of the data, although it has been reported that the overall glucose level, rather than the dose of insulin administered, directly influenced the outcome of patients (*3*).

Even with these limitations, we believe that our observation is still of value in considering the clinical impact of the strict control of hyperglycemia during the early phase of HSCT. To confirm our preliminary observation, a prospective pilot study is underway to assess the effect of intensive glucose control after HSCT. If this pilot study shows a beneficial effect of intensive glucose control, a prospective randomized trial would be warranted to confirm the possibility that intensive glucose control improves the outcome after HSCT. Additionally, in this ongoing pilot study, we evaluate the diurnal blood glucose and insulin levels, including postprandial levels, to detect hyperglycemia more precisely before transplantation since the level of HgA1c is affected by both the blood glucose level and the turnover rate of red blood cells, and would not precisely correlate with the true mean blood glucose level in patients who received courses of blood transfusion for anemia.

In conclusion, the association of the degree of hyperglycemia during neutropenia and an increased risk of post-transplant complications and NRM was suggested, but the possibility that intensive glucose control improves the outcome after HSCT would only be confirmed in a prospective randomized trial.

ACKNOWLEDGMENTS

We thank the medical, nursing, data processing, laboratory, and clinical staffs at the National Cancer Center Hospital for their important contributions to this study through dedicated care of the patients. The authors are indebted to Y. Iisaka and M. Kurita for their assistance with data collection. We also thank S. Saito for helping to prepare the manuscript.

REFERENCES

1. Van den Berghe G, Wouters P, Weekwrs F, et al. Intensive insulin therapy in the critically ill patients. *N Engl J Med* 2001; 345: 1359.
2. Van den Berghe G, Wilmer A, Hermans G, et al. Intensive insulin therapy in the medical ICU. *N Engl J Med* 2006; 354: 449.
3. Van den Berghe G, Wouters PJ, Bouillon R, et al. Outcome benefit of intensive insulin therapy in the critically ill: Insulin dose versus glycemic control. *Crit Care Med* 2003; 31: 359.
4. Krinsley JS. Association between hyperglycemia and increased hospital mortality in a heterogeneous population of critically ill patients. *Mayo Clin Proc* 2003; 78: 1471.
5. Krinsley JS. Effect of an intensive glucose management protocol on the mortality of critically ill adult patients. *Mayo Clin Proc* 2004; 79: 992.
6. Vogelzang M, Nijboer JM, van der Horst IC, et al. Hyperglycemia has a stronger relation with outcome in trauma patients than in other critically ill patients. *J Trauma* 2006; 60: 873.
7. Ingels C, Debaveye Y, Milants I, et al. Strict blood glucose control with insulin during intensive care after cardiac surgery: Impact on 4-years survival, dependency on medical care, and quality-of-life. *Eur Heart J* 2006; 27: 2716.
8. Jeschke MG, Klein D, Bolder U, Einspanier R. Insulin attenuates the systemic inflammatory response in endotoxemic rats. *Endocrinology* 2004; 145: 4084.
9. Brix-Christensen V, Andersen SK, Andersen R, et al. Acute hyperinsulinemia restrains endotoxin-induced systemic inflammatory response: An experimental study in a porcine model. *Anesthesiology* 2004; 100: 861.
10. Sheean PM, Freels SA, Helton WS, Braunschweig CA. Adverse clinical consequences of hyperglycemia from total parenteral nutrition exposure during hematopoietic stem cell transplantation. *Biol Blood Marrow Transplant* 2006; 12: 656.
11. Sheean PM, Braunschweig C, Rich E. The incidence of hyperglycemia in hematopoietic stem cell transplant recipients receiving total parenteral nutrition: A pilot study. *J Am Diet Assoc* 2004; 104: 1352.
12. Fietsam R Jr., Bassett J, Glover JL. Complications of coronary artery surgery in diabetic patients. *Am Surg* 1991; 57: 551.
13. Ortiz A, Ziyadeh FN, Neilson EG. Expression of apoptosis-regulatory genes in renal proximal tubular epithelial cells exposed to high ambient glucose and in diabetic kidney. *J Invest Med* 1997; 45: 50.
14. Vanhorebeek I, De Vos R, Mesotten D, et al. Protection of hepatocyte mitochondrial ultrastructure and function by strict blood glucose control with insulin in critically ill patients. *Lancet* 2005; 365: 53.
15. Przepiorka D, Weisdorf D, Martin P, et al. 1994 Consensus Conference on Acute GVHD Grading. *Bone Marrow Transplant* 1995; 15: 825.
16. Cavallo MG, Pozzilli P, Bird C, et al. Cytokines in sera from insulin-dependent diabetic patients at diagnosis. *Clin Exp Immunol* 1991; 86: 256.
17. Morohoshi M, Fujisawa K, Uchimura I, Numano F. Glucose-dependent interleukin 6 and tumor necrosis factor production by human peripheral blood monocytes in vitro. *Diabetes* 1996; 45: 954.
18. Borst SE. The role of TNF-alpha in insulin resistance. *Endocrine* 2004; 23: 177.
19. Esposito K, Nappo F, Marfella R, et al. Inflammatory cytokine concentrations are acutely increased by hyperglycemia in humans: Role of oxidative stress. *Circulation* 2002; 106: 2067.
20. Hotamisligil GS, Murray DL, Choy LN, Spiegelman BM. Tumor necrosis factor α inhibits signaling from the insulin receptor. *Proc Natl Acad Sci USA* 1994; 91: 4854.
21. Tsigos C, Papanicolaou DA, Kyrou I, et al. Dose-dependent effects of recombinant human interleukin-6 on glucose regulation. *J Clin Endocrinol Metab* 1997; 82: 4167.
22. Ferrara JL, Reddy P. Pathophysiology of graft-versus-host disease. *Semin Hematol* 2006; 43: 3.
23. Ferrara JL, Cooke KR, Teshima T. The pathophysiology of acute graft-versus-host disease. *Int J Hematol* 2003; 78: 181.
24. Teshima T, Ordemann R, Reddy P, et al. Acute graft-versus-host disease does not require alloantigen expression on host epithelium. *Nat Med* 2002; 8: 575.
25. Laster SM, Wood JG, Gooding LR. Tumor necrosis factor can induce both apoptotic and necrotic forms of cell lysis. *J Immunol* 1988; 141: 2629.
26. Schmaltz C, Alpdogan O, Muriglan SJ, et al. Donor T cell-derived TNF

is required for graft-versus-host disease and graft-versus-tumor activity after bone marrow transplantation. *Blood* 2003; 101: 2440.
27. Krenger W, Ferrara JL. Dysregulation of cytokines during graft-versus-host disease. *J Hematother* 1996; 5: 3.
28. Hiraoka A, Ohashi Y, Okamoto S, et al. Phase III study comparing tacrolimus (FK506) with cyclosporine for graft-versus-host disease prophylaxis after allogeneic bone marrow transplantation. *Bone Marrow Transplant* 2001; 28: 181.
29. Yanada M, Emi N, Naoe T, et al. Tacrolimus instead of cyclosporine used for prophylaxis against graft-versus-host disease improves outcome after hematopoietic stem cell transplantation from unrelated donors, but not from HLA-identical sibling donors: A nationwide survey conducted in Japan. *Bone Marrow Transplant* 2004; 34: 331.
30. Ratanatharathorn V, Nash RA, Przepiorka D, et al. Phase III study comparing methotrexate and tacrolimus (prograf, FK506) with methotrexate and cyclosporine for graft-versus-host disease prophylaxis after HLA-identical sibling bone marrow transplantation. *Blood* 1998; 92: 2303.
31. Webster AC, Woodroffe RC, Taylor RS, et al. Tacrolimus versus ciclosporin as primary immunosuppression for kidney transplant recipients: Meta-analysis and meta-regression of randomised trial data. *BMJ* 2005; 331: 810.
32. McAlister VC, Haddad E, Renouf E, et al. Cyclosporin versus tacrolimus as primary immunosuppressant after liver transplantation: a meta-analysis. *Am J Transplant* 2006; 6: 1578.
33. Woo M, Przepiorka D, Ippoliti C, et al. Toxicities of tacrolimus and cyclosporin A after allogeneic blood stem cell transplantation. *Bone Marrow Transplant* 1997; 20: 1095.
34. Margreiter R; European Tacrolimus vs Ciclosporin Microemulsion Renal Transplantation Study Group. Efficacy and safety of tacrolimus compared with ciclosporin microemulsion in renal transplantation: a randomised multicentre study. *Lancet* 2002; 359: 741.
35. Nash RA, Antin JH, Karanes C, et al. Phase 3 study comparing methotrexate and tacrolimus with methotrexate and cyclosporine for prophylaxis of acute graft-versus-host disease after marrow transplantation from unrelated donors. *Blood* 2000; 96: 2062.
36. Wingard JR, Nash RA, Przepiorka D, et al. Relationship of tacrolimus (FK506) whole blood concentrations and efficacy and safety after HLA-identical sibling bone marrow transplantation. *Biol Blood Marrow Transplant* 1998; 4: 157.
37. Przepiorka D, Nash RA, Wingard JR, et al. Relationship of tacrolimus whole blood levels to efficacy and safety outcomes after unrelated donor marrow transplantation. *Biol Blood Marrow Transplant* 1999; 5: 94.

Case Report

T-Cell Large Granular Lymphocyte Leukemia of Donor Origin After Cord Blood Transplantation

Shigeru Kusumoto, Shin-Ichiro Mori, Kisato Nosaka, Yuriko Morita-Hoshi, Yasushi Onishi, Sung-Won Kim, Takashi Watanabe, Yuji Heike, Ryuji Tanosaki, Yoichi Takaue, Kensei Tobinai

Abstract

We report the first case of T-cell large granular lymphocyte leukemia of donor origin after a second cord blood transplantation for acute myeloid leukemia, and review the literature regarding rare cases of T-cell–origin posttransplantation lymphoproliferative disorders.

Clinical Lymphoma & Myeloma, Vol. 7, No. 7, 475-479, 2007

Key words: Bone marrow, Epstein-Barr virus, Polymerase chain reaction, Posttransplantation lymphoproliferative disorders, T-cell receptor

Introduction

T-cell large granular lymphocyte leukemia (LGL; LGLL) is characterized by the monoclonal proliferation of $CD3^+$, and $CD8^+$ LGLs, with abundant cytoplasm and fine or coarse azurophilic granules.[1,2] Reactive expansion of LGL in the peripheral blood has been occasionally reported during viral infection and in recovery phase of allogeneic hematopoietic stem cell transplantation (HSCT).[3,4]

Posttransplantation lymphoproliferative disorder (PTLD) is a characteristic lymphoid proliferation or the development of lymphoma in a setting of decreased T-cell immune surveillance, typically in recipients of solid organ transplantation or allogeneic HSCT. Most reported cases of PTLD are of B-cell origin, in association with Epstein-Barr virus (EBV) infection, which leads to monoclonal or, less frequently, polyclonal proliferation of B cells. Most of the rare cases of T-cell PTLD were reported after solid organ transplantation, with very rare cases after allogeneic HSCT.

In this report, we describe the unique clinical and laboratory findings of a patient with γδ T-cell LGLL of cord donor origin after a second cord blood transplantation for acute myeloid leukemia.

Division of Hematology and Stem Cell Transplantation
National Cancer Center Hospital, Chuo-ku, Tokyo, Japan

Submitted: Sept 5, 2006; Revised: Dec 29, 2006; Accepted: Jan 18, 2007

Address for correspondence: Yoichi Takaue, MD, National Cancer Center Hospital, 5-1-1, Tsukiji, Chuo-ku, Tokyo 104-0045, Japan
Fax: 81-3-3542-3815; e-mail: ytakaue@ncc.go.jp

Case Report

A 58-year-old Japanese man with acute myeloid leukemia (French-American-British classification; M2) in second complete remission received allogeneic HSCT from an unrelated female cord blood donor. The conditioning regimen consisted of total body irradiation of 12 Gy in 6 fractions from day −6 to −4, and cyclophosphamide 60 mg/kg once daily intravenously on days −3 to −2 (total dose, 120 mg/kg). He received human leukocyte antigen–loci mismatched (2 by serology and 2 by DNA typing) unrelated cord blood, which contained 3.03×10^7 nucleated cells/kg in January 2003. Cyclosporine and short-term methotrexate were used as graft-versus-host disease prophylaxis. However, hematologic recovery was not observed up to day 40, and we concluded that this was a case of primary graft failure without leukemia relapse because the results of interphase fluorescence in situ hybridization analysis on days 23, 30, and 37 on bone marrow (BM) samples were negative. Because his condition remained good, we planned a second cord blood transplantation with a reduced-intensity regimen, which consisted of fludarabine 30 mg/kg once daily intravenously from days −8 to −3 (total dose 180 mg/kg), busulfan 4 mg/kg orally on days −6 and −5 (total dose 8 mg/kg), and total body irradiation of 4 Gy in 1 fraction on day −1. Cyclosporine and mycophenolate mofetil 15 mg/kg twice daily were administered. On day 51 of the initial transplantation in March 2003, human leukocyte antigen–loci mismatched (2 by serology and 3 by DNA typing) male cord blood, containing 2.6×10^7/kg nucleated cells, was infused. Neutrophil engraftment was observed by day 33 after second transplantation. Acute and chronic graft-versus-host disease did not develop, and cyclosporine was tapered off in November 2003.

ISSN #1532-2190;

Figure 1 T-Cell Large Granular Lymphocyte Leukemia Stained with May-Giemsa on the Peripheral Blood Smear

The predominant cells were typical of LGLs with abundant cytoplasm and fine or coarse azurophilic granules.
Hematoxylin and eosin stain; original magnification ×1000.

Figure 2 Southern Blots of T-Cell Receptor β-Chain Gene Rearrangements

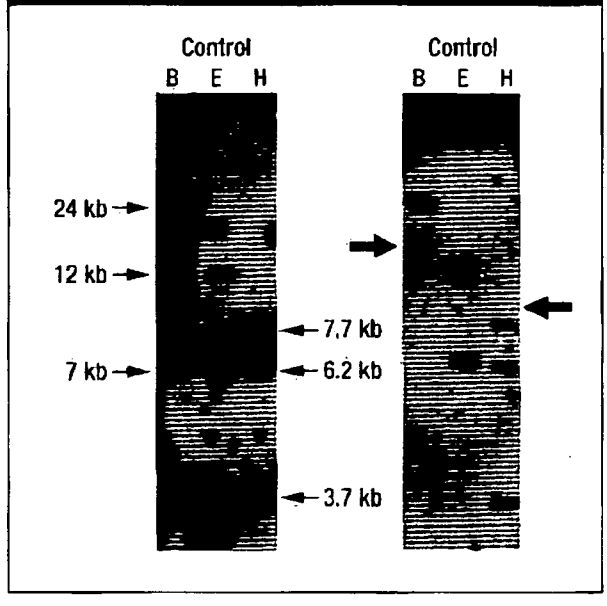

DNA from BM of this patient was hybridized with a TCR Cβ1 probe.
Arrows indicate rearranged bands.
Abbreviations: B = Bam H1; E = Eco R; H = Hind III

In February 2004, 10 months after the second cord blood transplantation, he developed anorexia, abdominal distention with fluid accumulation, and edema in the lower extremities. A computed tomography scan showed gross ascites and mild pleural effusion but no sign of enlarged lymph nodes or hepatosplenomegaly. The peripheral white blood cell count was 10,300/μL (10.3 × 10^9/L), and 30% of the cells had a morphology of medium to large lymphocytes with abundant azurophilic granules in the cytoplasm, as shown in Figure 1. The hemoglobin level was 8.8 g/dL (88 g/L), and the platelet count was 192 × 10^3/μL (1.92 × 10^9/L).

A retrospective review of the peripheral blood smears disclosed that the appearance of LGL coincided with the tapering off of immunosuppression 3 months before the admission.

Flow cytometry examination of the peripheral blood mononuclear cells showed a homogeneous population of T-cell LGLs positive for CD2, CD3, CD8, CD56, and T-cell receptor (TCR)–γδ, but negative for CD4 and TCR-αβ. The BM biopsy specimen histologically showed 10% of hypocellular gelatinous marrow with diffuse infiltration of medium to large lymphoid cells. Immunoperoxidase studies on sections of BM showed strong expression of T-cell–restricted intracellular antigen-1, partially positive staining of CD8 and granzyme B, but no expression of CD3 or CD20. Southern blot analysis of the BM cells revealed a clonal rearrangement of the TCR-β chain, as shown in Figure 2 and TCR-δ chain (data not shown).

Abdominal paracentesis was performed with milky chylous fluid, and a flow cytometry examination showed results similar to those in the peripheral blood. Multiprimer-based polymerase chain reaction (PCR) analysis of ascitic cells also showed clonal rearrangement of the TCR-δ chain, as shown in Figure 3. The primer sets were used in the following locations: Vδ1, 5'-AAA GTG GTC GCT ATT CTG TC-3'; Vδ2A, 5'-GCA CCA TCA CAG AGA GAT GA-3'; Jδ, 5'- TGG TTC CAC AGT CAC ACG GG-3'; Dδ3B, 5'-TTG TAC CAC CGT GCG TAT CC-3'. The amplified 200 base-pair PCR products of the TCR-δ chain were then cloned into the pCR-TOPO vector. The DNA sequences of 3 clones amplified by vectors were identical and had high homology to TCR-δ chain including a 197 base-pair sequence (data not shown). This sequence also involved the forward and reverse primers Vδ1 and Jδ, respectively, described previously.

The results of all of the previously mentioned studies indicated the clonal expansion of T cells compatible with a diagnosis of T-cell LGLL with γδ T-cell phenotype involving peripheral blood, BM, and ascites.

Donor-recipient DNA chimerism was analyzed by comparing the short tandem repeat findings for the donor blood sample and pretransplantation recipient samples. Eleven short tandem repeat loci were analyzed by PCR using an AmpFISTR SGM Plus® kit. The peripheral blood sample (containing 30% T-LGL) and the second cord blood sample showed the same peaks at the locus (D16S539), as shown in Figure 4. These results further confirmed that the expanded γδ T-LGL cells were exclusively of second cord blood transplantation donor origin.

Serologic examination showed no evidence of viral infection. Real-time PCR analysis revealed a high load of EBV (7.9 × 10^3 copies/10^6 cells). However, in situ hybridization studies of BM cells did not reveal EBV-encoded small RNA, and Southern blot analysis of BM cells also showed no band for